



ELSEVIER

Contents lists available at ScienceDirect

# Transportation Research Part E

journal homepage: [www.elsevier.com/locate/tre](http://www.elsevier.com/locate/tre)

## Modeling cascade dynamics of railway networks under inclement weather

Dali Wei <sup>a,1</sup>, Hongchao Liu <sup>b,\*</sup>, Yong Qin <sup>c,2</sup><sup>a</sup> Civil and Environmental Engineering Department, University of California Davis, 1 Shields Ave, Davis, CA 95616, United States<sup>b</sup> Civil and Environmental Engineering Department, Texas Tech University, 10th and Akron, Lubbock, TX 79409, United States<sup>c</sup> State Key Laboratory of Rail Traffic Control and Safety, Beijing Jiaotong University, Beijing, China

### ARTICLE INFO

#### Article history:

Received 16 April 2014

Received in revised form 2 April 2015

Accepted 5 May 2015

#### Keywords:

Railway delay

Railway schedule

Timetable

Vulnerability

Robustness

### ABSTRACT

Understanding the cascade dynamics of delay propagation under inclement weather is crucial to proactive railway management. In this paper, we proposed a Switching Max-Plus System (SMPS) to model the delay propagation on railway networks, which extends the conventional MPS by incorporating multiple system matrices to capture the dynamic impacts of inclement weather. An algorithm based on the All-Paired Critical-Path (APCP) graph was developed to solve the SMPS, which calculates secondary delays without backtracking the precedent events. The proposed model and its solution algorithm were validated using discrete-time simulations on both artificial and empirical networks. The robustness of railway services was also analyzed using the concepts of vulnerability and diffusivity.

© 2015 Elsevier Ltd. All rights reserved.

## 1. Introduction

Recently, with the rapid development of rail infrastructure, the railway system is becoming one of the busiest transportation modes in China with over 1.4 billion trips taken every year (Chou et al., 2011; Zheng, 2010). As China's railway network spans through numerous diverse climate regions, its operation is always subject to inclement weather, such as strong rainstorms and blizzards. Under such conditions, the operating speed is constrained by the Rail Transportation Weather Index (RTWI) and relevant safety regulations (China Meteorological Administration, 2007). The reduction in operating speed may result in severe primary and secondary delays over the entire railway network (Cui and Zhang, 2010; Ma et al., 2011; Zeng et al., 2012). For example, on February 4th 2013, due to snowstorms in northern China, three major railway services among Beijing, Tianjin, Shanghai, and Guangzhou suffered from severe delays; some services were even canceled, leaving thousands of passengers stranded in Shanghai Station for over three hours. On December 15th 2012, more than 10 high-speed rail services from Beijing Station were delayed for nearly 2 h in the morning due to heavy fog and snowstorms. The operating speed was reduced from 300 to 100 km per hour (km/h), resulting in severe primary and knock-on delays over the network.

Although the delay caused by severe weather is inevitable, understanding the underlying cascade dynamics of delay propagation is crucial for the effective management of a railway network. Due to the shared infrastructural resources, the primary delay of an arrival or departure may propagate to its subsequent events. Such propagation of train delays at the

\* Corresponding author. Tel.: +1 (806)7422801; fax: +1 (806)7424168.

E-mail addresses: [dlwei@ucdavis.edu](mailto:dlwei@ucdavis.edu) (D. Wei), [hongchao.liu@ttu.edu](mailto:hongchao.liu@ttu.edu) (H. Liu), [yqin@bjtu.edu.cn](mailto:yqin@bjtu.edu.cn) (Y. Qin).

<sup>1</sup> Tel.: +1 (806)4519416.

<sup>2</sup> Tel.: +86 57211625.

network scale could be rather complicated and often exhibits a cascade pattern, where the delay of a single service may lead to a catastrophic cascade of delays over the entire network (Zhou and Zhong, 2007).

Usually, train delays are grouped into two categories: the primary delay and the secondary (knock-on) delay. The primary delay is directly caused by incidents such as the malfunctioning of the infrastructure and inclement weather. The secondary delay, on the other hand, is due to the propagation of delays incurred by other services because of track sharing, operational constraints, and safety regulations such as the minimum running headway and speed limit (Kliewer and Suhl, 2011).

To capture the propagation of primary delays, several stochastic delay models have been developed with the objective of estimating stationary distributions of secondary delays. For instance, Carey and Kwiecinski (1994) investigated multiple train services on single-track lines with stochastic running and dwell times. Probability density functions of successive arrival and departure times were derived in a recursive way. Higgins and Kozan (1998) presented another stochastic delay model of urban railway networks, where they assumed that source delays were due to frequent random events (e.g., long dwell times) and followed certain distributions (e.g., the Erlang distribution). An implicit expression was proposed to derive the expectations of secondary delays. Recently, Meester and Muns (2007) extended the model by using phase-type distributions. The objective of these stochastic models was to derive the stationary distributions of train delays given the primary delays that follow certain probability distributions. Since inclement weather is a type of small probability event, these stochastic models can only provide statistical properties of train delays in the long run. They are unable to predict train delays when the network is affected by inclement weather with a specific spatial–temporal coverage. Therefore, it is unfeasible to compare these stochastic models with the proposed method due to the different modeling objectives and applicable scenarios.

In contrast to stochastic models, the deterministic approach applies the max-plus algebra, wherein movements of trains are depicted as a discrete-event system. For example, Braker (1993) developed a recursive system using the max-plus algebra for periodic timetables of the Dutch railway network. Subiono (2000) extended Braker's model to accommodate networks with mixed train types. Based on these Max-Plus System (MPS) models, De Schutter et al. (2002) and van den Boom and De Schutter (2006) proposed several control models to reschedule train services for mitigating secondary delays.

However, these static MPS models (Braker, 1993; De Schutter et al., 2002; Goverde, 2007; Subiono, 2000) can only be applied in situations when initial delays are known and their propagation is governed by static constraints in normal conditions. When railway networks suffer from inclement weather that changes in both temporal and spatial scales, the constraints are no longer static; instead, they evolve accordingly to time. Delay propagation exhibits a more intricate pattern. On the one hand, additional primary delays may be coupled into the system while earlier primary delays are still propagating. In this case, the propagation of earlier delays no longer follows normal regulations, and therefore, a single system matrix with normal constraints is insufficient. On the other hand, even if the weather condition is assumed static, primary delays still cannot be readily obtained as dependencies may exist among primary delays themselves.

In this paper, we present a Switching Max-Plus System (SMPS) to model the delay propagation under the dynamic impact of inclement weather. In contrast to existing MPS methods, the SMPS introduces a system matrix for each operation scenario, describing the impacts of the inclement weather at different stages. The railway network is switching between different operating modes with the dynamics of hazardous weather. An algorithm based on the All-Paired Critical-Path (APCP) graph is developed to solve the SMPS and has two main advantages: first, it enables a direct calculation of the delay of a certain event without the need of backtracking its precedent events; second, measures of service robustness, such as vulnerability and diffusivity, can be readily determined from the APCP graph. For a comparison, an iterative algorithm is also presented based on the precedence graph of the slack time matrix. Case studies on both artificial and empirical networks are conducted to validate the model and its solution algorithm.

The proposed model contributes to the state-of-the-art railway operation research in two ways: (1) it successfully modeled the delay propagation through an SMPS approach. SMPS is a significant extension of MPS, in which the structure of SMPS is not constant but rather evolving with time. To the best knowledge of the authors, very few, if any, studies have taken into account the dynamics of constraints (inclement weather, in this study) in modeling the delay evolution in railway networks; and (2) an APCP graph based algorithm was developed to replace the iterative approach for improving the computational efficiency. More importantly, robustness measures of railway services, i.e., the vulnerability and the diffusivity, can be derived from the APCP graph.

The rest of the paper is organized as follows. Section 2 presents the SMPS model for delay propagation under inclement weather. Section 3 proposes the APCP algorithm for solving the SMPS model, as well as robustness measures derived from the APCP graph. Section 4 presents cases studies on both artificial and empirical railway networks. Section 5 concludes the paper.

## 2. Model formulation

In this section, we first define the problem and introduce the basic notation. Then, the fundamentals of the max-plus algebra are presented. We demonstrate how operational constraints of a railway system can be expressed using the max-plus algebra. Then, we propose a Switching MPS (SMPS) approach for modeling the cascade dynamics of railway networks under the impacts of inclement weather.

## 2.1. Problem statement

A railway network is represented by an undirected multigraph, in which the nodes of the graph represent stations denoted by  $\mathbf{V} = \{v_1, \dots, v_{n_v}\}$ , where  $n_v$  is the number of stations. The edges of the graph represent rail links between stations denoted by  $\mathbf{L} = \{l_1, \dots, l_{n_l}\}$ , where  $n_l$  is the number of links. The route of a train is specified by a sequence of adjacent links from the origin to the destination.<sup>3</sup> The scheduled arrival and departure times are denoted by an  $n_e \times 1$  column vector  $\mathbf{T}$ , where  $n_e$  is the total number of arrivals and departures.<sup>4</sup> Assume that train operations are subject to multi-stage inclement weather. In each stage (time interval), the inclement weather has a certain spatial coverage and affects a subset of links with different levels of intensity. Operating speeds on these links have to be reduced to certain thresholds based on safety rules defined in RTWI. The objective of the proposed model is to determine the primary and secondary delays of each arrival and departure, considering the dynamic impacts of the multi-stage inclement weather. Basic variables and parameters are listed in Table 1. Other notation used for definitions and theorems are explained in the context.

## 2.2. Max-plus algebra

The max-plus algebra is a mathematical approach that can be used to describe a discrete event system. This section outlines the fundamentals of the max-plus algebra. We refer to Baccelli et al. (1992) and Butkovic (2010) for a systematic introduction.

Usually, the max-plus algebra is introduced as follows. Let  $\epsilon = -\infty$  and  $e = 0$ . For elements  $a, b \in \mathbb{R}_{\max}$  where  $\mathbb{R}_{\max} = \mathbb{R} \cup \epsilon$ , the operations  $\oplus$  and  $\otimes$  are defined as:

$$a \otimes b = a + b \quad (1)$$

$$a \oplus b = \max(a, b) \quad (2)$$

$$a \oplus \epsilon = \epsilon \oplus a = a \quad (3)$$

$$a \otimes \epsilon = \epsilon \otimes a = \epsilon \quad (4)$$

$$a \otimes e = e \otimes a = a \quad (5)$$

Let  $\mathbb{R}_{\max}^{n \times n}$  denote the set of  $n \times n$  matrices with entries in  $\mathbb{R}_{\max}$ . The matrix multiplication and addition are defined as:

$$[\mathbf{P} \otimes \mathbf{Q}]_{ij} = \bigoplus_{k=1}^n (p_{ik} \otimes q_{kj}) = \max_{k=1, \dots, n} (p_{ik} + q_{kj}) \quad (6)$$

$$[\mathbf{P} \oplus \mathbf{Q}]_{ij} = (p_{ij} \oplus q_{ij}) \quad (7)$$

where  $\mathbf{P}, \mathbf{Q} \in \mathbb{R}_{\max}^{n \times n}$ . The  $k$ th ( $k \geq 1$ ) power of  $\mathbf{P}$  is defined as:

$$\mathbf{P}^k = \otimes_{i=1}^k \mathbf{P} \quad (8)$$

In the max-plus algebra, an  $n \times n$  matrix can be uniquely associated with a precedence graph, which is defined as:

**Definition 1** Baccelli et al., 1992. The precedence graph  $G(\mathbf{P})$  associated to a matrix  $\mathbf{P} \in \mathbb{R}_{\max}^{n \times n}$  is a weighted digraph  $G = (\Gamma, \mathbf{E}, \omega)$  with  $\Gamma = \{1, \dots, n\}$  and an arc  $(j, i) \in \mathbf{E}$  with weight  $\omega(j, i) = p_{ij}, p_{ij} \neq \epsilon$ .

**Definition 2.** A path  $\Psi$  in  $G(\mathbf{P})$  is a sequence of adjacent arcs  $\Psi = (\zeta_1, \dots, \zeta_m), (m \geq 1)$  such that the head of  $\zeta_i$  is the tail of  $\zeta_{i+1}, (0 \leq i \leq m-1)$ . The length of a path  $\Psi$  is the number of arcs it contains. The weight of the path is the sum of the arc weights, i.e.,  $\gamma(\Psi) = \otimes_{\zeta_i \in \Psi} \omega_i$ , where  $\omega_i$  is the weight of arc  $\zeta_i$ . Letting  $\zeta_i^+$  and  $\zeta_i^-$  denote the head and the tail of  $\zeta_i$ , respectively, a path  $\Psi$  can also be specified as  $\Psi = (\zeta_1^-, \dots, \zeta_m^+)$ .

## 2.3. Max-plus system for a railway network

In this section, we introduce the MPS model to lay a logical ground for the later development of the SMPS approach. As a scheduled system, railway operations are subjected to several constraints such as minimum arrival and departure headways. Using the max-plus algebra, these constraints are expressed as follows.

**Running time constraint:** the travel time between two successive stations cannot be smaller than the minimum running time determined by the speed limit. Let  $t_{v,r,0}$  and  $x_{v,r,0}$  be the scheduled and actual arrival times of train  $r$  at station  $v$ , respectively. Let  $x_{v',r,1}$  denote the actual departure time of train  $r$  at station  $v'$  (i.e., the preceding station of  $v$  on the route of train  $r$ ). This running time constraint can be expressed by Eq. (9). Here,  $j$  denotes the link that connects station  $v'$  and  $v$ .  $M_{r,j}$  is the minimum running time of train  $r$  on link  $j$ .

<sup>3</sup> Multiple links may exist between two stations. Therefore, specifying the route of a train using the sequence of links is more precise than using a sequence of stations.

<sup>4</sup> The elements of  $\mathbf{T}$  do not need to be arranged in a specific order as long as the order is consistent throughout the system.

**Table 1**  
List of variables and parameters.

Notation	Description
<i>Notation used for describing operational constraints</i>	
$t_{v,r,0}$	Scheduled arrival time of train $r$ at station $v$
$t_{v,r,1}$	Scheduled departure time of train $r$ at station $v$
$x_{v,r,0}$	Actual arrival time of train $r$ at station $v$
$x_{v,r,1}$	Actual departure time of train $r$ at station $v$
$v'_r$	Preceding station of train $r$ at station $v$
$M_{r,l}$	Minimum travel time of train $r$ on link $l$
$\eta_{r,l}$	Travel time of train $r$ on link $l$ without considering the impacts of inclement weather
$h_{r_a,r_b,v}^{(0)}$	Minimum headway between arrivals of train $r_a$ and $r_b$ at station $v$
$h_{r_a,r_b,v}^{(1)}$	Minimum headway between departures of train $r_a$ and $r_b$ at station $v$
$h_{r_a,r_b,v}^{(2)}$	Safety time at station $v$ between the departure of train $r_a$ and the arrival of train $r_b$
$h_{r,v}^{(3)}$	Minimum dwell time of train $r$ at station $v$
$s_{r,l}^{(H)}$	Maximum operating speed of train $r$ on link $l$ in normal conditions
$s_{r,l}^{(0)}$	Operating speed of train $r$ on link $l$ in normal conditions
$\mathbf{A}_{n_e \times n_e}^{(0)}$	System matrix in normal conditions with entries $a_{ij}^{(0)}, i, j = 1, \dots, n_e$
$\mathbf{B}_{n_e \times n_e}^{(0)}$	Slack time matrix in normal conditions with entries $b_{ij}^{(0)}, i, j = 1, \dots, n_e$
$\mathbf{C}_{n_e \times n_e}$	APCP matrix with entries $c_{ij}, i, j = 1, \dots, n_e$
<i>Notation used for describing inclement weather and its impacts on train operations</i>	
$\beta_k^-$	Starting time of stage $k$
$\beta_k^+$	Ending time of stage $k$
$N_\beta$	Total number of time intervals (stages) of inclement weather
$s_{r,l}^{(k)}$	Maximum operating speed of train $r$ on link $l$ under inclement weather at stage $k$
$\mathbf{A}_{n_e \times n_e}^{(k)}$	System matrix at stage $k$ with entries $a_{ij}^{(k)}, i, j = 1, \dots, n_e$
$\mathbf{B}_{n_e \times n_e}^{(k)}$	Slack time matrix at stage $k$ with entries $b_{ij}^{(k)}, i, j = 1, \dots, n_e$
$\mathbf{D}_{n_e \times 1}$	Delay vector with entries $d_i, i = 1, \dots, n_e$
$\mathbf{X}_{n_e \times 1}$	Vector of actual times of events with entries $x_i, i = 1, \dots, n_e$

$$x_{v,r,0} = (M_{r,j} \otimes x_{v',r,1}) \oplus t_{v,r,0} \quad (9)$$

*Arrival headway constraint:* if train  $r_a$  and  $r_b$  have the same inbound route at station  $v$  and if  $r_b$  is scheduled to depart after  $r_a$ , their arrival headway cannot be smaller than a minimum constant  $h_{r_a,r_b,v}^{(0)}$ . This can be expressed as:

$$x_{v,r_b,0} = (h_{r_a,r_b,v}^{(0)} \otimes x_{v,r_a,0}) \oplus t_{v,r_b,0} \quad (10)$$

*Departure headway constraint:* assuming that two trains,  $r_a$  and  $r_b$ , have the same outbound route at station  $v$ , if  $r_b$  is scheduled to depart after  $r_a$ , their departure headway cannot be smaller than a minimum constant  $h_{r_a,r_b,v}^{(1)}$ . This can be expressed as:

$$x_{v,r_b,1} = (h_{r_a,r_b,v}^{(1)} \otimes x_{v,r_a,1}) \oplus t_{v,r_b,1} \quad (11)$$

*Safety time at stations:* two trains,  $r_a$  and  $r_b$ , are assumed to share the same platform at station  $v$ . The arrival of  $r_b$  is scheduled after the departure of  $r_a$ . The headway between the departure of  $r_a$  and the arrival of  $r_b$  cannot be smaller than a minimum constant  $h_{r_a,r_b,v}^{(2)}$ . This is expressed as:

$$x_{v,r_b,0} = (h_{r_a,r_b,v}^{(2)} \otimes x_{v,r_a,1}) \oplus t_{v,r_b,0} \quad (12)$$

*Dwell time constraint:* the departure of train  $r$  at the station  $v$  cannot be earlier than  $h_{r,v}^{(3)}$  time units after its arrival, which can be expressed as:

$$x_{v,r,1} = (h_{r,v}^{(3)} \otimes x_{v,r,0}) \oplus t_{v,r,1} \quad (13)$$

Let  $\mathbf{A}_{n_e \times n_e}$  denote the set of constraint elements corresponding to a set of  $n_e$  events. The scheduled times of the events are denoted by a vector of  $\mathbf{T}_{n_e \times 1}$ , while the realized arrival and departure times are represented by  $\mathbf{X}_{n_e \times 1}$ . For example, letting  $t_i = t_{v,r,1}$ ,  $x_j = x_{v,r,0}$  and  $x_i = x_{v,r,1}$ , Eq. (13) can be rewritten as:

$$x_i = (a_{ij} \otimes x_j) \oplus t_i \quad (14)$$

where  $a_{ij} = h_{r,v}^{(3)}$ . If the punctuality of event  $i$  does not depend on event  $j$ , then  $a_{ij} = \epsilon$ . For periodic timetables, let  $x_i(\kappa)$  denote the actual time of event  $i$  at period  $\kappa$  ( $\kappa \geq 0$ ). By extending Eq. (14), Goverde (2007) developed an MPS for periodic timetables in the form of:

$$\mathbf{X}(\kappa) = \mathbf{A} \otimes \mathbf{X}(\kappa) \oplus \mathbf{T} \oplus \mathbf{X}(\kappa^-) \quad (15)$$

where  $\mathbf{X}(\kappa^-)$  represents actual times of events before the propagation of delays at period  $\kappa$ . Primary delays, if any, are included in  $\mathbf{X}(\kappa^-)$  for the propagation in period  $\kappa$ . The precedence graph of the system matrix  $\mathbf{A}$  indicates the dependencies among the events. If there exists an arc from node  $j$  to  $i$ , i.e.,  $a_{ij} \neq \epsilon$ , then event  $i$  depends on event  $j$  and the earliest possible time of event  $i$  is  $a_{ij}$  time units after event  $j$  occurs.

To understand Eq. (15), below we give a simple example. Assume the system only involves one period and contains two events: the departure of a train at a station and its arrival at the next station. The minimum travel time is assumed to be 100 min. This constraint is satisfied by the following equation:

$$\begin{bmatrix} x_1 \\ x_2 \end{bmatrix} = \mathbf{A} \otimes \begin{bmatrix} x_1 \\ x_2 \end{bmatrix} = \begin{bmatrix} e & \epsilon \\ 100 & e \end{bmatrix} \otimes \begin{bmatrix} x_1 \\ x_2 \end{bmatrix} \quad (16)$$

where  $x_1$  and  $x_2$  are the actual departure and arrival times, respectively. From Eq. (16), we obtain  $x_2 \geq x_1 + 100$ , and there exist infinitely many solutions. However, the actual times cannot be earlier than the scheduled times  $\mathbf{T}$ , so Eq. (16) needs to be expanded to:

$$\begin{bmatrix} x_1 \\ x_2 \end{bmatrix} = \mathbf{A} \otimes \begin{bmatrix} x_1 \\ x_2 \end{bmatrix} \oplus \mathbf{T} = \begin{bmatrix} e & \epsilon \\ 100 & e \end{bmatrix} \otimes \begin{bmatrix} x_1 \\ x_2 \end{bmatrix} \oplus \begin{bmatrix} t_1 \\ t_2 \end{bmatrix} \quad (17)$$

where  $t_1$  and  $t_2$  are the scheduled departure and arrival times, respectively. The solutions of Eq. (17) are  $x_2 = \max(t_1 + 100, t_2)$  and  $x_1 = t_1$ , which satisfy both the travel time constraint and the schedule. Now, we assume that the departure has incurred a primary delay of 5 min, which can be incorporated into the system as:

$$\begin{bmatrix} x_1 \\ x_2 \end{bmatrix} = \begin{bmatrix} e & \epsilon \\ 100 & e \end{bmatrix} \otimes \begin{bmatrix} x_1 \\ x_2 \end{bmatrix} \oplus \begin{bmatrix} t_1 \\ t_2 \end{bmatrix} \oplus \begin{bmatrix} t_1 + 5 \\ t_2 \end{bmatrix} \quad (18)$$

The solutions of Eq. (18) are then  $x_1 = t_1 + 5$  and  $x_2 = \max(t_1 + 105, t_2)$ . If the scheduled arrival time is larger than  $t_1 + 105$ , then the actual arrival time is the same as the scheduled time, i.e.,  $x_2 = t_2$ . Otherwise, the arrival would incur a secondary delay of  $t_1 + 105 - t_2$ .

In the following discussions, we do not explicitly integrate periods for cyclic timetables, i.e., events of cyclic services in different periods are treated as if they were acyclic. On one hand, it would simplify the SMPS model and allow less complex algorithms in delay prediction. On the other hand, it is also easy to transform periodic to non-periodic timetables using the unfolding technique, where the dependency between events in different periods is still reserved (Goverde, 2007; van der Meer, 2008). Additionally, partially periodic and non-periodic train services are also being adopted in practical train operations in Europe and China to cope with the non-uniformly distributed demand and exceptional situations, where the non-periodic expression would be applicable (Caimi et al., 2011; Forsgren et al., 2011; Wong et al., 2008; Canca et al., 2014; Cacchiani et al., 2014).

#### 2.4. Modeling cascade dynamics of railway network under inclement weather

As one can identify in Eq. (15), the static MPS adopts a constant matrix  $\mathbf{A}$  to define operational constraints in normal conditions. Primary delays are assumed to propagate based on these static constraints. However, due to the dynamic impacts of inclement weather, operational constraints are expected to evolve accordingly. In such cases, the delay propagation cannot be predicted using the static MPS.

In this section, we propose the SMPS model, where the system matrix is switching among different operation modes based on the intensity of the inclement weather. It is assumed that the inclement weather spans over  $N_\beta$  ( $N_\beta \geq 1$ ) stages. At each stage, the inclement weather has a certain spatial coverage and affects a subset of links with different levels of intensity. A system matrix is determined for each stage to represent the operational constraints. Therefore, there exist  $N_\beta + 1$  system matrices including one normal system matrix and  $N_\beta$  abnormal system matrices  $\mathbf{A}^{(k)}$  ( $i = 1, \dots, N_\beta$ ) corresponding to each stage of the inclement weather. To simplify the expression below, let  $\mathbf{A}^{(0)}$  denote the system matrix in normal conditions. The following max-plus system is proposed to incorporate multiple system matrices:

$$\mathbf{X}(t) = \mathbf{A}^{(\phi(t))} \otimes \mathbf{X}(t) \oplus \mathbf{T} \oplus \mathbf{X}(t^-) \quad (19)$$

where  $\mathbf{X}(t)$  denotes the actual times of events at time  $t$ .  $\mathbf{X}(t^-)$  denotes the actual times of events that are already known at time  $t$ .  $\phi(t) = 0, 1, 2, \dots, N_\beta$  is the index of the corresponding system matrix at time  $t$ . Let  $\beta_k^-$  denote the starting time and  $\beta_k^+$  the ending time of stage  $k$  ( $k = 1, \dots, N_\beta$ ). If  $t \in [\beta_k^-, \beta_k^+]$ , then  $\mathbf{A}^{(\phi(t))} = \mathbf{A}^{(k)}$ . Eq. (19) establishes a multilevel MPS model with a dynamic system matrix that switches between different operation modes. We take the previous example used for Eq. (15) to explain Eq. (19). The departure is also assumed to incur a 5-min primary delay, but the minimum travel time increases to 150 min due to the inclement weather at stage  $k$ . Based on Eq. (19), we have:

$$\begin{bmatrix} x_1 \\ x_2 \end{bmatrix} = \mathbf{A}^{(k)} \otimes \begin{bmatrix} x_1 \\ x_2 \end{bmatrix} \oplus \begin{bmatrix} t_1 \\ t_2 \end{bmatrix} \oplus \begin{bmatrix} t_1 + 5 \\ t_2 \end{bmatrix} = \begin{bmatrix} e & \epsilon \\ 150 & e \end{bmatrix} \otimes \begin{bmatrix} x_1 \\ x_2 \end{bmatrix} \oplus \begin{bmatrix} t_1 \\ t_2 \end{bmatrix} \oplus \begin{bmatrix} t_1 + 5 \\ t_2 \end{bmatrix} \quad (20)$$

The solutions of Eq. (20) are  $x_1 = t_1 + 5$  and  $x_2 = \max(t_1 + 155, t_2)$ . If the scheduled arrival time is larger than  $t_1 + 155$ , then the actual arrival time is the same as the scheduled time, i.e.,  $x_2 = t_2$ . Otherwise, the arrival would incur a delay equal to  $t_1 + 155 - t_2$ .

Now, we need to determine constraint elements in  $\mathbf{A}^{(k)}$ . In the  $k$ th stage, the speed limit on an affected link  $l$  has to be reduced to  $s_{r,l}^{(k)} < s_{r,l}^{(0)}$ . Here,  $s_{r,l}^{(0)}$  is the operating speed of train  $r$  on link  $l$  in normal conditions and  $s_{r,l}^{(k)}$  is the maximum operating speed at stage  $k$ . Moreover, let  $s_{r,l}^H$  denote the speed limit in normal conditions for train  $r$  on link  $l$ .

To facilitate the derivation below, let  $x_j$  denote the actual departure time of train  $r$  at station  $v_r$  and  $x_i$  the corresponding arrival time at station  $v_r$ . If the departure event  $j$  is delayed by  $d_j$  ( $d_j \geq 0$ ) time units, then the travel time of train  $r$  on link  $l$  is:

$$\eta_{r,l} = \begin{cases} \zeta_l/s_{r,l}^{(0)} - d_j & d_j + \frac{\zeta_l}{s_{r,l}^H} - \frac{\zeta_l}{s_{r,l}^{(0)}} \leq 0 \\ \zeta_l/s_{r,l}^H & d_j + \frac{\zeta_l}{s_{r,l}^H} - \frac{\zeta_l}{s_{r,l}^{(0)}} > 0 \end{cases} \quad (21)$$

where  $\zeta_l$  is the length of link  $l$ . As illustrated in Fig. 1a, the first case in Eq. (21) indicates that the departure delay  $d_j$  is recovered due to the difference between the maximum speed and the normal speed. The arrival event  $i$  is still punctual and the travel time is  $\zeta_l/s_{r,l}^{(0)} - d_j$ . In the other case shown in Fig. 1b, the train has to travel at the maximum speed on the entire link and the travel time is  $\zeta_l/s_{r,l}^H$ .

If  $x_j \geq \beta_k^+$  or  $x_j \leq \beta_k^- - \eta_{r,l}$ , the arrival event  $i$  is not affected by the inclement weather at stage  $k$ , and therefore,  $a_{ij}^{(k)} = a_{ij}^{(0)}$ . However, if  $\beta_k^- \leq x_j < \beta_k^+$ , then the departure event  $j$  happens after stage  $k$  starts. The constraint element  $a_{ij}^{(k)}$  is given as:

$$a_{ij}^{(k)} = \begin{cases} \zeta_l/s_{r,l}^{(k)} & s_{r,l}^{(k)}(\beta_k^+ - x_j) \geq \zeta_l \\ \beta_k^+ - x_j + (\zeta_l - (\beta_k^+ - x_j)s_{r,l}^{(k)})/s_{r,l}^H & s_{r,l}^{(k)}(\beta_k^+ - x_j) < \zeta_l \end{cases} \quad (22)$$

As shown in Fig. 2a, the first case in Eq. (22) represents the scenario that the train has arrived at station  $v_r$  before stage  $k$  ends, and the minimum travel time is then  $\zeta_l/s_{r,l}^{(k)}$ . The second case indicates that the train is still traveling on link  $l$  when stage  $k$  ends, and therefore, the train operates at the maximum speed  $s_{r,l}^H$  on the remaining segment of link  $l$ . The minimum travel time is then  $\beta_k^+ - x_j + (\zeta_l - (\beta_k^+ - x_j)s_{r,l}^{(k)})/s_{r,l}^H$  as shown in Fig. 2b.

If  $\beta_k^- - \eta_{ij} < x_j < \beta_k^-$ , then the departure event  $j$  happens before stage  $k$  starts. In this case, the train has already traveled a distance of  $\zeta_l'$ :

$$\zeta_l' = \begin{cases} s_{r,l}^H(\beta_k^- - x_j) & d_j + \frac{\zeta_l}{s_{r,l}^H} - \frac{\zeta_l}{s_{r,l}^{(0)}} > 0 \\ s_{r,l}^H \min\left(\frac{s_{r,l}^{(0)}d_j}{s_{r,l}^H - s_{r,l}^{(0)}}, \beta_k^- - x_j\right) + s_{r,l}^{(0)} \max\left(\beta_k^- - x_j - \frac{s_{r,l}^{(0)}d_j}{s_{r,l}^H - s_{r,l}^{(0)}}, 0\right) & d_j + \frac{\zeta_l}{s_{r,l}^H} - \frac{\zeta_l}{s_{r,l}^{(0)}} \leq 0 \end{cases} \quad (23)$$

The first case in Eq. (23) indicates that the train has to travel at the maximum speed on the entire link to compensate the departure delay  $d_j$ . Therefore, when stage  $k$  starts, the train has traveled a distance of  $s_{r,l}^H(\beta_k^- - x_j)$  as illustrated in Fig. 3a.

In the second case, the train only needs to travel at the maximum speed for a period of  $s_{r,l}^{(0)}d_j / (s_{r,l}^H - s_{r,l}^{(0)})$  as shown in Fig. 3b. If  $\beta_k^- - x_j$  is less than  $s_{r,l}^{(0)}d_j / (s_{r,l}^H - s_{r,l}^{(0)})$ , then the train has traveled a distance of  $s_{r,l}^H(\beta_k^- - x_j)$  when stage  $k$  starts.

Otherwise,  $\zeta_l'$  is the sum of the distance traveled at the maximum speed, i.e.,  $s_{r,l}^H \frac{s_{r,l}^{(0)}d_j}{s_{r,l}^H - s_{r,l}^{(0)}}$ , and the distance traveled at the normal speed, i.e.,  $s_{r,l}^{(0)}\left(\beta_k^- - x_j - \frac{s_{r,l}^{(0)}d_j}{s_{r,l}^H - s_{r,l}^{(0)}}\right)$ . Given  $\zeta_l'$  from Eq. (23), the constraint element in this scenario can be determined as:

$$a_{ij}^{(k)} = \begin{cases} (\zeta_l - \zeta_l')/s_{r,l}^{(k)} + (\beta_k^- - x_j) & \zeta_l' + s_{r,l}^{(k)}(\beta_k^- - \beta_k^+) \geq \zeta_l \\ (\zeta_l - \zeta_l' - s_{r,l}^{(k)}(\beta_k^- - \beta_k^+))/s_{r,l}^H + (\beta_k^- - x_j) & \zeta_l' + s_{r,l}^{(k)}(\beta_k^- - \beta_k^+) < \zeta_l \end{cases} \quad (24)$$

In Eq. (24), the first case indicates the train has arrived at station  $v_k$  before stage  $k$  ends as shown in Fig. 4a. After stage  $k$  starts, the train has to lower the speed to  $s_{r,l}^{(k)}$  for the remaining segment of the link, i.e.,  $\zeta_l - \zeta_l'$ . The minimum travel time is then  $(\zeta_l - \zeta_l')/s_{r,l}^{(k)} + (\beta_k^- - x_j)$ . The second case in Eq. (24) corresponds to the scenario that the train is still traveling on link  $l$  when stage  $k$  ends. As illustrated in Fig. 4b, the train operates at the maximum speed  $s_{r,l}^H$  on the remaining segment of link  $l$  after stage  $k$  ends. Therefore, the minimum travel time in this case is  $(\zeta_l - \zeta_l' - s_{r,l}^{(k)}(\beta_k^- - \beta_k^+))/s_{r,l}^H + (\beta_k^- - x_j)$ .

Now we define matrix  $\mathbf{B}^{(k)}$  as the slack time matrix with its entries being:

$$b_{ij}^{(k)} = t_j + a_{ij}^{(k)} - t_i \quad (25)$$

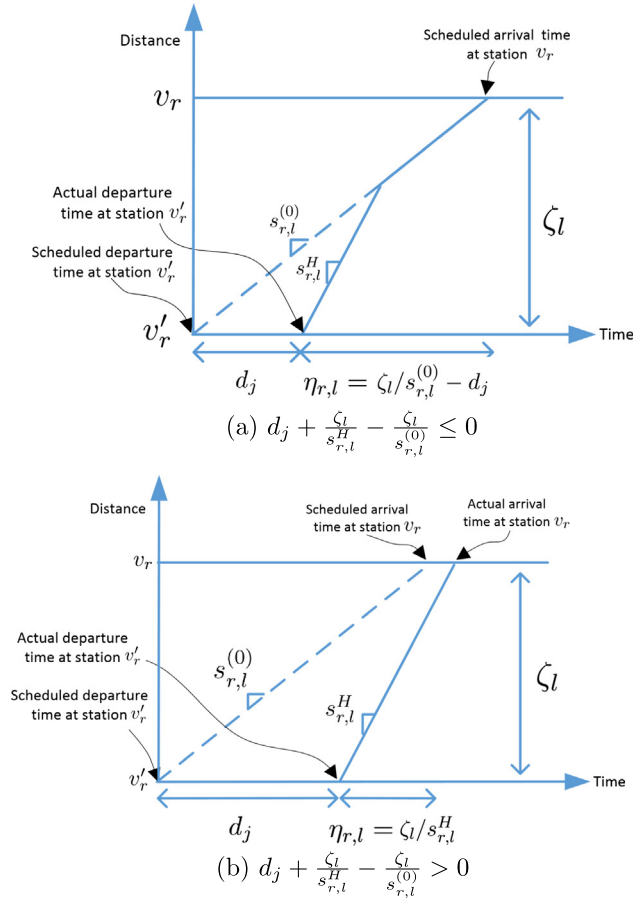


Fig. 1. Graphical illustration of the calculation of  $\eta_{r,l}$  using Eq. (21).

Using the slack time matrix would allow us to reformulate the SMPS so that delays can be directly incorporated into the system. Because  $a_{ij}^{(k)}$  represents the minimum time interval between event  $i$  and event  $j$ ,  $b_{ij}^{(k)}$  indicates the slack time between the scheduled and earliest possible time of event  $i$ . Given a timetable that satisfies all the constraints, we have  $b_{ij}^{(0)} \leq 0$  and  $b_{ij}^{(k)} \geq b_{ij}^{(0)}$ . If  $b_{ij}^{(k)} > 0$ , event  $i$  will incur a primary delay, and  $d_i$  is larger than  $d_j$ . Otherwise,  $d_j$  will be mitigated due to the negative slack time. From Eq. (25), the SMPS Eq. (19) can be transformed into a system represented by the delay and the slack time matrix as:

$$\mathbf{D}(t) = \mathbf{B}^{(\phi(t))} \otimes \mathbf{D}(t) \oplus \mathbf{0} \oplus \mathbf{D}(t^-) \tag{26}$$

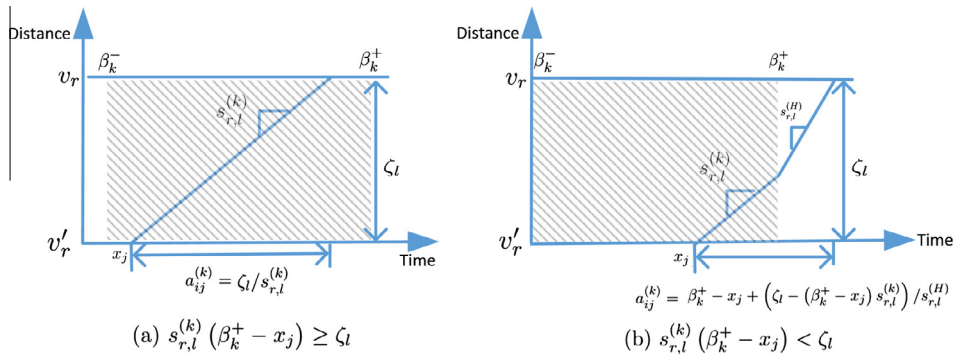


Fig. 2. Graphical illustration of the calculation of  $a_{ij}^{(k)}$  using Eq. (22).

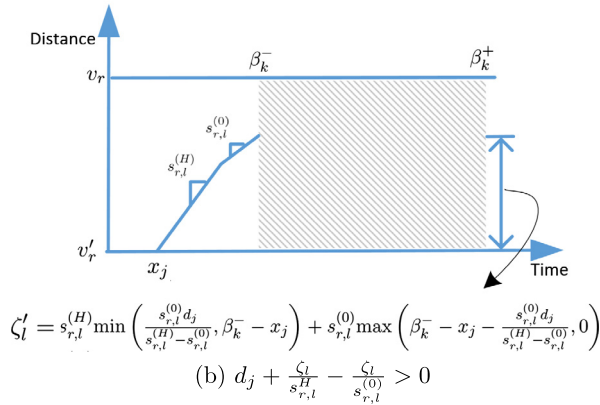
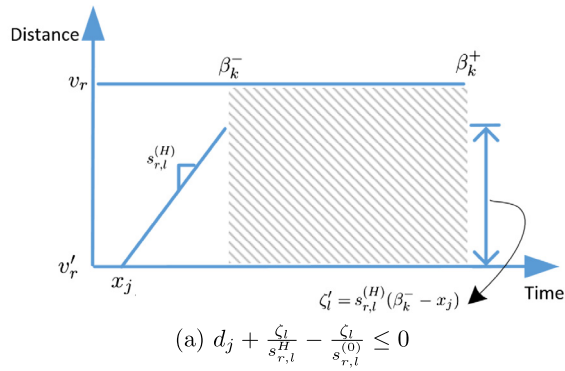


Fig. 3. Graphical illustration of the calculation of  $\zeta_l'$  using Eq. (23).

where  $\mathbf{D}(t)$  is the  $n_e \times 1$  delay vector with the entries being the delays of arrivals and departures at time  $t$ .  $\mathbf{D}(t^-)$  denotes delays of events that are known at time  $t$ .  $\mathbf{0}$  is the zero matrix in the max-plus algebra. If  $t \in [\beta_k^-, \beta_k^+]$ , then  $\mathbf{B}^{(\phi(t))} = \mathbf{B}^{(k)}$ . Eq. (26) can be interpreted using the same example for Eq. (19). Assuming the scheduled travel time is  $t_2 - t_1 = 140$  min, the slack time between the arrival and departure at stage  $k$  is then  $t_2 + 150 - t_1 = 10$  min. Based on Eq. (26), we have:

$$\begin{bmatrix} d_1 \\ d_2 \end{bmatrix} = \mathbf{B}^{(k)} \otimes \begin{bmatrix} d_1 \\ d_2 \end{bmatrix} \oplus \begin{bmatrix} e \\ e \end{bmatrix} \oplus \begin{bmatrix} 5 \\ e \end{bmatrix} = \begin{bmatrix} e & \epsilon \\ 10 & e \end{bmatrix} \otimes \begin{bmatrix} d_1 \\ d_2 \end{bmatrix} \oplus \begin{bmatrix} e \\ e \end{bmatrix} \oplus \begin{bmatrix} 5 \\ e \end{bmatrix} \tag{27}$$

Hence,  $d_1 = 5$  and  $d_2 = d_1 + 10 = 15$ , which indicates that the arrival of the train incurs a 15-min delay. The same results can also be obtained by taking  $t_2 - t_1 = 140$  into Eq. (20).

### 3. Solution algorithm

To solve the SMPS defined in Eq. (26), an intuitive approach would be an iterative algorithm, which rearranges the events in a topological order and calculates the actual times based on their precedent events. This algorithm is presented in Section 3.3. However, the iterative algorithm has an obvious drawback. Calculating the delay of a certain event requires that all its precedent ones have to be visited. In this section, we propose the All-Paired Critical-Path (APCP) algorithm that enables a direct calculation of any secondary delay without backtracking the precedent events.

#### 3.1. The All-Paired Critical-Path (APCP) algorithm

In the precedence graph  $G(\mathbf{B}^{(0)})$ , if a path  $\Psi = (q_n, \dots, q_1), n > 1$  exists from node  $q_n$  to  $q_1$ , we call the operation in Eq. (28) a tracing operation from  $q_n$  to  $q_1$  on path  $\Psi$ :

$$\left( \otimes_{i=1}^{n-1} b_{q_i q_{i+1}}^{(0)} \right) \otimes d_{q_n} \oplus 0 \tag{28}$$

where  $d_{q_n}$  is the delay of event  $q_n$ . Here,  $\left( \otimes_{i=1}^{n-1} b_{q_i q_{i+1}}^{(0)} \right)$  is termed as the Cumulative Slack Time (CST) of path  $\Psi$ .

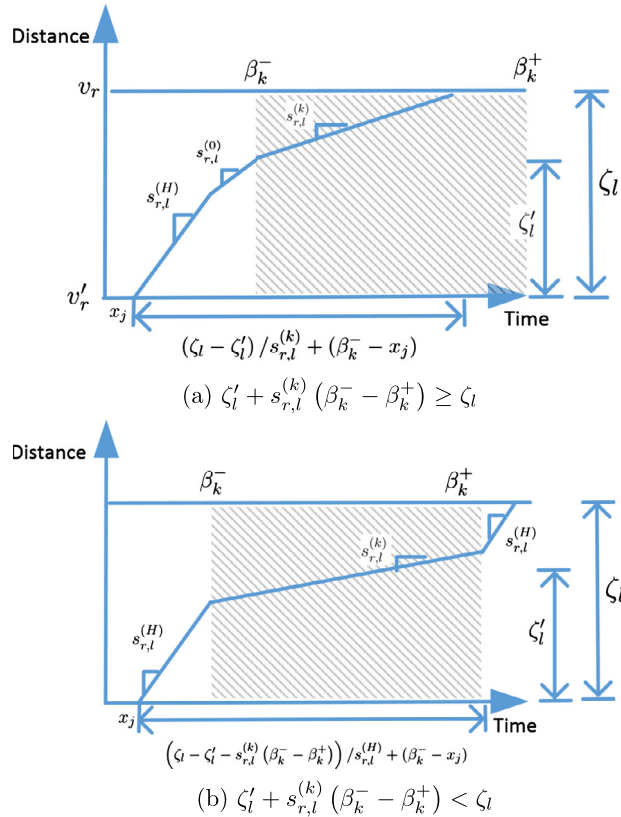


Fig. 4. Graphical illustration of the calculation of  $d_{ij}^{(k)}$  using Eq. (24).

**Definition 3.** If there exists more than one path from node  $q_n$  to node  $q_0$  in the precedence graph  $G(\mathbf{B}^{(0)})$ , then the critical path is defined as the path with the largest weight.

**Definition 4.** Let  $P(q) = \{p_k\}, k = 1, 2, 3 \dots, n$  denote a set of events with primary delays of  $d_{p_k}$ , where each event connects to node  $q (q \notin P)$  with a critical path  $\{q_k^{(m_k)}, q_k^{(m_k-1)}, \dots, q_k^{(1)}, q_k^{(0)}\} (q_k^{(0)} = q \text{ and } q_k^{(m_k)} = p_k)$ . Then, the Critical Primary Event (CPE) of event  $q$ , denoted by  $p_q^{(C)}$ , is defined as:

$$p_q^{(C)} = \arg \max_{p_k \in P(q)} \left( \left( \otimes_{j=0}^{m_k-1} b_{q_i^{(j)} q_i^{(j+1)}}^{(0)} \right) \otimes d_{p_k} \right) \tag{29}$$

With the preparation of Definitions 3 and 4, we give the following theorem.

**Theorem 1.** The secondary delay of any arrival or departure event can be determined by a tracing operation to its CPE on the critical path.

**Proof.** Let  $C_i$  denote the set of the precedent nodes of event  $i$ . If  $j \in C_i$ , then we have  $b_{ij}^{(0)} \neq \epsilon$ . From Eq. (25), one obtains:

$$d_i = b_{iq_i^{(1)}}^{(0)} \otimes d_{q_i^{(1)}} \oplus 0 \tag{30}$$

where

$$q_i^{(1)} = \arg \max_{j \in C_i} (b_{ij}^{(0)} \otimes d_j) \tag{31}$$

To facilitate the derivation below, we let  $q_i^{(0)}$  denote  $i$ . Recursively applying Eq. (30) until  $d_{q_i^{(m)}} (m \geq 1)$  is a primary delay, we have:

$$d_i = \left( \otimes_{j=1}^m b_{q_i^{(j-1)} q_i^{(j)}}^{(0)} \right) \otimes d_{q_i^{(m)}} \oplus 0 \tag{32}$$

Eq. (32) is a tracing operation from  $q_i^{(m)}$  to  $q_i^{(0)}$  on path  $\Psi = \{q_i^{(m)}, \dots, q_i^{(0)}\}$ . To prove Theorem 1, one needs to show: (1)  $\Psi$  is the critical path from  $q_i^{(m)}$  to  $i$  and (2)  $q_i^{(m)}$  is the CPE of  $i$ .

Assume  $\{w_i^{(n)}, \dots, w_i^{(0)}\}$  with  $w_i^{(n)} = q_i^{(m)}$  and  $w_i^{(0)} = i$  is another path from  $q_i^{(m)}$  to  $i$ . From Eq. (31), one obtains:

$$b_{iq_i^{(1)}}^{(0)} \otimes d_{q_i^{(1)}} \geq b_{iw_i^{(1)}}^{(0)} \otimes d_{w_i^{(1)}} \geq \left( \otimes_{j=1}^n b_{w_i^{(j-1)} w_i^{(j)}}^{(0)} \right) \otimes d_{q_i^{(m)}} \tag{33}$$

Taking Eqs. (30) and (32) into Eq. (33), we have:

$$\left( \otimes_{j=1}^m b_{q_i^{(j-1)} q_i^{(j)}}^{(0)} \right) \otimes d_{q_i^{(m)}} \geq \left( \otimes_{j=1}^n b_{w_i^{(j-1)} w_i^{(j)}}^{(0)} \right) \otimes d_{q_i^{(m)}} \tag{34}$$

Hence,

$$\otimes_{j=1}^m b_{q_i^{(j-1)} q_i^{(j)}}^{(0)} \geq \otimes_{j=1}^n b_{w_i^{(j-1)} w_i^{(j)}}^{(0)} \tag{35}$$

Eq. (35) shows that  $\Psi = \{q_i^{(m)}, \dots, q_i^{(0)}\}$  is the path with the largest weight, and therefore, it is the critical path from  $q_i^{(m)}$  to  $i$ .

Now, we need to prove that  $q_i^{(m)}$  is the CPE of  $i$ . Let  $\mathbf{P}(i) = \{p_k\}$  ( $k = 1, 2, 3, \dots, n$ ) denote the set of events with primary delays of  $d_{p_k}$ . Each event in  $\mathbf{P}(i)$  connects to  $i$  with a critical path  $\{q_k^{(m_k)}, q_k^{(m_k-1)}, \dots, q_k^{(1)}, q_k^{(0)}\}$  ( $q_k^{(0)} = i$  and  $q_k^{(m_k)} = p_k$ ). From Eq. (31), one obtains the following inequality:

$$b_{iq_k^{(1)}}^{(0)} \otimes d_{q_k^{(1)}} \geq b_{iq_k^{(1)}}^{(0)} \otimes d_{q_k^{(1)}} \tag{36}$$

Because  $\{q_k^{(m_k)}, q_k^{(m_k-1)}, \dots, q_k^{(1)}, q_k^{(0)}\}$  is the critical path from  $q_k^{(m_k)}$  to  $q_k^{(0)}$ , the right hand side of Eq. (36) equals to:

$$b_{iq_k^{(1)}}^{(0)} \otimes d_{q_k^{(1)}} = \left( \otimes_{j=1}^{m_k-1} b_{q_k^{(j-1)} q_k^{(j)}}^{(0)} \right) \otimes d_{q_k} \tag{37}$$

Taking Eqs. (32) and (36) into Eq. (37), one obtains:

$$\left( \otimes_{j=1}^m b_{q_i^{(j-1)} q_i^{(j)}}^{(0)} \right) \otimes d_{q_i^{(m)}} \geq \left( \otimes_{j=1}^{m_k-1} b_{q_k^{(j-1)} q_k^{(j)}}^{(0)} \right) \otimes d_{q_k} \tag{38}$$

Therefore,

$$q_i^{(m)} = \arg \max_{p_k \in \mathbf{P}(i)} \left( \left( \otimes_{j=1}^{m_k-1} b_{q_k^{(j-1)} q_k^{(j)}}^{(0)} \right) \otimes d_{q_k} \right) \tag{39}$$

and  $q_i^{(m)}$  is the CPE of event  $i$ . This completes the proof of Theorem 1. □

According to Theorem 1, to determine the secondary delay of any arrival or departure event, one only needs to find the delay of its CPE and the CST of the critical path. Now, let's define an all-paired critical-path graph to determine the critical paths between the events.

**Definition 5.** The all-paired critical-path graph associated with the precedence graph  $G(\mathbf{B}^{(0)})$  is a weighted digraph  $G_s = (\Gamma, \mathbf{E}, \omega_s)$  with  $\Gamma = \{1, 2, \dots, n_e\}$  and an arc  $(j, i) \in \mathbf{E}$ . The weight of an arc  $(j, i)$  equals the weight of the critical path from  $j$  to  $i$  in the precedence graph, i.e.,  $\omega_s(j, i) = \gamma(\Psi_{j,i})$  where  $\Psi_{j,i}$  is the critical path from  $j$  to  $i$  in  $G(\mathbf{B}^{(0)})$ . If there is no path from  $j$  to  $i$ , then  $\omega_s(j, i) = \epsilon$ .

Based on the APCP graph, we define the APCP matrix  $\mathbf{C}$  with the entries being  $c_{ij} = \omega_s(j, i)$ ,  $i, j = 1, 2, \dots, n_e$ . Using the arc weight of the APCP graph, Eq. (32) can be written as:

$$d_i = w_s(q_i^{(m)}, i) \otimes d_{q_i^{(m)}} \oplus 0 \tag{40}$$

where  $q_i^{(m)}$  satisfies Eq. (39). Combining Eqs. (39) and (40), we have:

$$d_i = \left( \oplus_{p_k \in \mathbf{P}(i)} w_s(p_k, i) \otimes d_{p_k} \right) \oplus 0 \tag{41}$$

where  $\mathbf{P}$  is the set of primary delays. Eq. (41) is the central result of the algorithm, which states that only primary delays and arc weights on the APCP graph are required for determining secondary delays.

Based on Eq. (41), the APCP algorithm is programmed into two parts. In the first part, primary delays are calculated based on slack time matrices at different stages. Then, by using Eq. (41), all the secondary delays can be readily determined. The pseudo-code is illustrated in Fig. 5. Row( $p_1$ ) indicates the index of event  $p_1$  in  $\mathbf{X}$ . Ar( $p_1$ ) represents the arrival event of departure  $p_1$ . At each stage, we first determine a set of possible departures whose outbound links will be affected by the increment

weather. This is implemented in function  $\text{Depart}(\mathbf{I}^{(k)})$ . If the departure occurs before stage  $k$  ends, the actual time of its arrival is updated by using the constraints at stage  $k$ . If the arrival delay is caused by the inclement weather at stage  $k$  instead of the propagation of primary delays, it will be added into  $\mathbf{Q}$  as a new primary delay. Once primary delays are determined, secondary delays can be simply obtained using Eq. (41).

Base on the iteration structure, the time complexity of the APCP algorithm is:

$$\mathcal{T}_{\text{APCP}}(n_e, N_\beta) = \mathcal{O}(N_\beta n_e) \quad (42)$$

where  $n_e$  is the number of events and  $N_\beta$  is the number of stages. The merit of the algorithm is that, when determining a secondary delay, the backtracking operation is avoided. If we change the sign of arc weights, the APCP graph can be easily generated from the precedent graph  $G(\mathbf{B}^{(0)})$  by well-known shortest-path graph algorithms, such as the Floyd–Warshall algorithm (Floyd, 1962; Warshall, 1962) or the Johnsons algorithm (Johnson, 1977). Since  $\mathbf{B}^{(0)}$  is a typical sparse matrix, the Johnsons algorithm would be less time-consuming than the Floyd–Warshall algorithm.

### 3.2. Identification of vulnerability and diffusivity using the APCP graph

As shown in the previous section, the APCP algorithm enables a direct calculation of any secondary delay without backtracking the precedent events. Moreover, the APCP graph also explicitly indicates the vulnerability and diffusivity of each arrival and departure event in a railway network.

If a certain arrival or departure is closely related to other events, a small primary delay can result in a large amount of secondary delays over the entire network. We call this departure or arrival highly diffusive.

**Definition 6.** Let  $d_k^{(d_i)}$  denote the secondary delay of event  $k$  given a primary delay  $d_i = d^*$  incurred by event  $i$ . Let  $\mathbf{H}_i$  denote the set of events excluding event  $i$ . The diffusivity of event  $i$  at intensity  $d^*$  is defined as the sum of secondary delays it causes over the entire network, i.e.,  $F_i(d^*) = \otimes_{k \in \mathbf{H}_i} d_k^{(d_i)}$ .

The diffusivity can be readily determined from  $G_s(\mathbf{B}^{(0)})$  as:

$$F_i(d^*) = \otimes_{k \in \mathbf{H}_i} (\omega_s(i, k) \otimes d^* \oplus 0) \quad (43)$$

The diffusivity measures an event's capability to propagate the primary delay incurred by itself to other events. A highly diffusive event can be viewed as a hub in the precedence graph, whose punctuality is critical to the entire network. From Eq. (43), one can find that:

$$d^* \leq -\oplus_{k \in \mathbf{H}_i} \omega_s(i, k) \rightarrow F_i(d^*) = 0 \quad (44)$$

Here,  $-\oplus_{k \in \mathbf{H}_i} \omega_s(i, k)$  indicates the maximum absorptive capacity of event  $i$ . If  $d^*$  is less than this threshold, it can be absorbed by event  $i$  and will not cause any knock-on delays. Otherwise,  $d^*$  will be spread to other events.

If a certain event heavily relies on the punctuality of other events, a small primary delay incurred by other events may easily propagate to and affect this event. We call this event highly vulnerable.

**Definition 7.** Let  $d_i^{(d_k)}$  denote the secondary delay of event  $i$  given a primary  $d_k = d^*$  incurred by event  $k$ . The vulnerability is defined as the sum of secondary delays incurred by  $i$  if a primary delay happens to any other event in the network, i.e.,  $U_i(d^*) = \otimes_{k \in \mathbf{H}_i} d_i^{(d_k)}$ , where  $\mathbf{H}_i$  is the set of all events excluding  $i$ .

A high vulnerability means the event is more likely to be affected by a primary delay incurred by an arbitrary event in the network. Using the APCP graph, the vulnerability of event  $i$  can be derived as:

$$U_i(d^*) = \oplus_{k \in \mathbf{H}_i} (\omega_s(k, i) \otimes d^* \oplus 0) \quad (45)$$

From Eq. (43), one can find that:

$$d^* \leq -\oplus_{k \in \mathbf{H}_i} \omega_s(k, i) \rightarrow U_i(d^*) = 0 \quad (46)$$

Here,  $-\oplus_{k \in \mathbf{H}_i} \omega_s(k, i)$  indicates the maximum primary delay event  $i$  can resist. If  $d^*$  is less than this threshold, event  $i$  will not be affected. Otherwise, event  $i$  would incur a secondary delay.

Diffusivity and vulnerability measure the robustness of railway services from two complementary perspectives. Vulnerability measures the capability to resist the primary delay, while diffusivity indicates the capability to propagate the primary delay to other events. The vulnerability of an event depends on the inbound arcs of its corresponding node on the APCP graph. Reducing the weights of its inbound arcs, i.e., increasing slack times regarding its precedent events, would diminish its vulnerability. On the other hand, the diffusivity of an event depends on the outbound arcs. Reducing the weights of the outbound arcs, i.e., increasing the slack times with respect to its subsequent events, would lower its diffusivity due to the increased absorptive threshold defined in Eq. (44).

Therefore, the role of an event in delay propagation can be viewed as a filter, where only severe primary delays can pass and propagate. The capability of the filter can be quantified using two thresholds derived from Eqs. (44) and (46). The first threshold is the same as the absorptive capacity defined in (46):

**Input:**

$\mathbf{T} = \mathbf{X}_{n_e \times 1}^{(0)}$ : scheduled times for all events;  $\mathbf{I}^{(k)}, l = 1, \dots, N_\beta$ : the set of affected links at each stage;  $G_s(\mathbf{B}^{(0)})$ : APCP graph of  $\mathbf{B}^{(0)}$ .

**Intermediate variables:**

$\mathbf{Q} = \{q_1, q_2, \dots\}$ : the set of events with primary delays;  $\mathbf{P} = \{p_1, p_2, \dots\}$ : candidate departures to be affected by inclement weather.

**Output:**  $d_i$  of event  $i$ 

```

1: for  $l = 1; l \leq N_\beta; l++$  do
2:    $\mathbf{P} = \text{Depart}(\mathbf{I}^{(k)})$ 
3:   while  $\mathbf{P}$  is not empty do
4:      $r = \text{Row}(p_1)$ 
5:      $d_r = \oplus_{j \in \mathbf{Q}} (\omega_s(j, r) \otimes d_j) \oplus 0$ 
6:     if  $d_r + t_r < \beta_k^+$  then
7:        $u = \text{Row}(\text{Ar}(p_1))$ 
8:        $d'_u = \oplus_{j \in \mathbf{Q}} (\omega_s(j, u) \otimes d_j) \oplus 0$ 
9:       if  $d'_u + t_u > \beta_k^-$  then
10:        Determine  $b_{ur}^{(k)}$  according to Eqs. (21) to (24)
11:         $d_u = (d_r \otimes b_{ur}^{(k)}) \otimes 0$ 
12:        Insert  $u$  into  $\mathbf{Q}$ 
13:      end if
14:      Remove  $p_1$  from  $\mathbf{P}$ 
15:    end if
16:  end while
17: end for
18: for each  $i \notin \mathbf{Q}$  do
19:    $d_i = (\oplus_{j \in \mathbf{Q}} \omega_s(j, i) \otimes d_j) \oplus 0$ 
20: end for

```

Fig. 5. The APCP algorithm.

$$\Theta_{low} = -\oplus_{k \in \mathbf{H}_i} \omega_s(i, k) \quad (47)$$

It is impossible for any primary delay to affect event  $i$  if it is smaller than this threshold. The second threshold is:

$$\Theta_{high} = -\oplus_{k \in \mathbf{H}_i} \omega_s(k, i) - \oplus_{k \in \mathbf{H}_i} \omega_s(i, k) \quad (48)$$

If the primary delay is less than  $\Theta_{high}$ , it may affect event  $i$  but cannot be propagated further to any subsequent event. Those two thresholds provide importation information to evaluate the severity of a primary delay with respect to a subsequent event. As long as the primary delay is less than  $\Theta_{high}$ , the delay propagation can be eliminated for any subsequent event of  $i$ . It is noteworthy that the diffusivity and vulnerability are two different measures. They do not have explicit relations. The diffusivity cannot be determined from the vulnerability, and vice versa. Given the same primary delay, for some events, the diffusivity is higher than the vulnerability (e.g., the event highly relies on the punctuality of other events, but it has little impact on its subsequent events), while for others, it may not.

### 3.3. Iterative algorithm

For comparison purposes, we also present an iterative algorithm in this section. The basic idea is to backtrack the precedent events through expanding the precedence graph  $G(\mathbf{B}^{(0)})$ . The details of the algorithm is given in Fig. 6.

At each stage, a set of departure and arrival events are determined that are likely to be affected by the inclement weather. This is implemented in function Candidate( $\mathbf{I}^{(k)}$ ). If it is an arrival event, its delay will be determined using the system matrix at stage  $k$ . Then, all its precedent nodes are visited to ensure all the constraints are satisfied. Any subsequent event that depends on this arrival will be updated as well. After primary delays are determined, calculations of secondary delays are implemented by backtracking its precedent nodes. The algorithm is carefully designed in a chronological order so that before calculating the delay of a certain event, its precedent events have already been visited. The time complexity of the iterative algorithm is:

$$\mathcal{T}_{\text{Iterative}}(n_e, N_\beta) = \mathcal{O}(N_\beta n_e^2) \quad (49)$$

Compared with Eq. (42), the iterative algorithm is obviously more time-consuming than the APCP algorithm because each precedent event has to be visited to determine a secondary delay.

**Input:**  $\mathbf{T}_{n_e \times 1} = \mathbf{X}_{n_e \times 1}^{(0)}$ : scheduled times for all events;  $\mathbf{I}^{(k)}, l = 1, \dots, N_\beta$ : the intensity of inclement weather;  $G(\mathbf{B}^{(0)})$ : precedence graph  $\mathbf{B}^{(0)}$ .

**Output:**  $d_i$  of event  $i$

```

1: for  $l = 1; l \leq N_\beta; l++$  do
2:    $\mathbf{P} = \text{Candidate}(\mathbf{I}^{(k)}) \cup \mathbf{Q}$ 
3:   while  $\mathbf{P}$  is not empty do
4:      $u = \text{Row}(p_1)$ 
5:     if  $u$  is an arrival event then
6:        $r = \text{Row}(\text{De}(p_1))$ 
7:       Determine  $b_{ur}^{(k)}$  according to Eqs. (21) to (24)
8:        $d_u = d_r \otimes b_{ur}^{(k)} \oplus 0$ 
9:     end if
10:    for each  $j$  in  $\text{Precede}(u), j \neq r$  do
11:       $d_u = d_j \otimes b_{ur}^{(0)} \oplus d_u$ 
12:    end for
13:    if  $d_u > 0$  then
14:      if  $u$  is an arrival event or ( $u$  is a departure event and  $d_u + t_u \leq \beta_k^+$ ) then
15:        Add  $\text{Depend}(p_1)$  into  $\mathbf{P}$ 
16:      else
17:        Add  $\text{Depend}(p_1)$  into  $\mathbf{Q}$ 
18:      end if
19:    end if
20:  end while
21: end for
22: while  $\mathbf{Q}$  is not empty do
23:    $u = \text{Row}(q_1)$ 
24:   for each  $j$  in  $\text{Precede}(u), j \neq r$  do
25:      $d_u = d_j \otimes b_{uj}^{(0)} \oplus d_u$ 
26:   end for
27:   if  $d_u > 0$  then
28:     Add  $\text{Depend}(q_1)$  to  $\mathbf{Q}$ 
29:   end if
30:   Remove  $q_1$  from  $\mathbf{Q}$ 
31: end while

```

Fig. 6. Iterative algorithm.

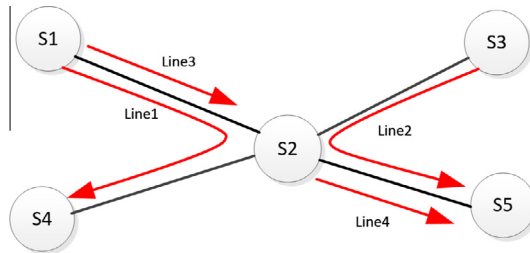


Fig. 7. An artificial network.

## 4. Experiments and discussions

In this section, case studies are presented on both an artificial and a real network. The purpose of the experiments is two-fold. First, the proposed model and the solution algorithm, i.e., the APCP algorithm, are validated using a discrete-time simulation program. The description and workflow of the simulation program are provided in Appendix A. Second, the robustness of the arrival and departure events in both networks are analyzed in terms of diffusivity and vulnerability.

### 4.1. Case study on an artificial network

A small tractable network is designed, which includes five stations and four services, as shown in Fig. 7. The link length between stations is 166 km. The minimum travel time on each link is 100 min. The speed limit in normal conditions is assumed to be 100 km/h. The minimum departure headway, the minimum arrival headway, the safety time at stations,

**Table 2**  
Timetable of the artificial network.

Service 1	Service 2	Service 3	Service 4
Arrival at S1: 8:10( $x_1$ )	Arrival at S3: 8:45( $x_3$ )	Arrival at S1: 9:50( $x_5$ )	Arrival at S2: 12:40( $x_{13}$ )
Departure at S1: 8:20( $x_2$ )	Departure at S3: 8:55( $x_4$ )	Departure at S1: 10:00( $x_6$ )	Departure at S2: 12:45( $x_{14}$ )
Arrival S2: 10:20( $x_7$ )	Arrival at S2: 10:55( $x_9$ )	Arrival at S2: 11:50( $x_{11}$ )	Arrival at S5: 14:45( $x_{16}$ )
Departure at S2: 10:35( $x_8$ )	Departure at S2: 11:10( $x_{10}$ )		
Arrival at S4: 12:35( $x_{12}$ )	Arrival at S5: 13:10( $x_{15}$ )		

**Table 3**  
Train delays under the acyclic timetable (in minutes).

Events	Simulation results	Iterative algorithm	APCP algorithm
Service 1 Arrival at Station 2 (Primary delay)	155	155	155
Service 1 Departure at Station 2	145	145	145
Service 2 Arrival at Station 2	130	130	130
Service 2 Departure at Station 2	120	120	120
Service 3 Arrival at Station 2 (Primary delay)	85	85	85
Service 1 Arrival at Station 4	125	125	125
Service 4 Arrival at Station 2	45	45	45
Service 4 Departure at Station 2	40	40	40
Service 2 Arrival at Station 5 (Primary delay)	187	187	187
Service 4 Arrival at Station 5 (Primary delay)	97	97	97

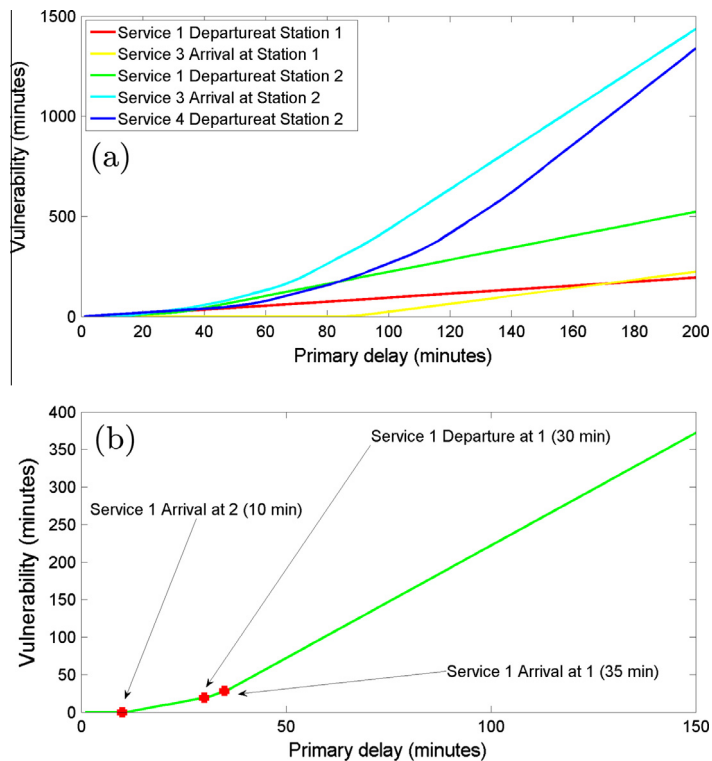


**Fig. 8.** (a) Vulnerabilities of arrivals and departures in the artificial railway network and (b) vulnerability of the departure of service 1 at station 2.

and the minimum dwell time are assumed to be 5 min. Moreover, we assume these train services share the same platforms at stations. Suppose the network is subjected to a two-stage inclement weather event. The first stage begins at 8:00 and ends at 12:00, during which the maximum operating speed on the link between station 1 and station 2 has to be reduced to 30 km/h. The second stage begins at 12:00 and ends at 15:00, during which the maximum operating speed on the link between station 2 and station 5 has to be reduced to 30 km/h.

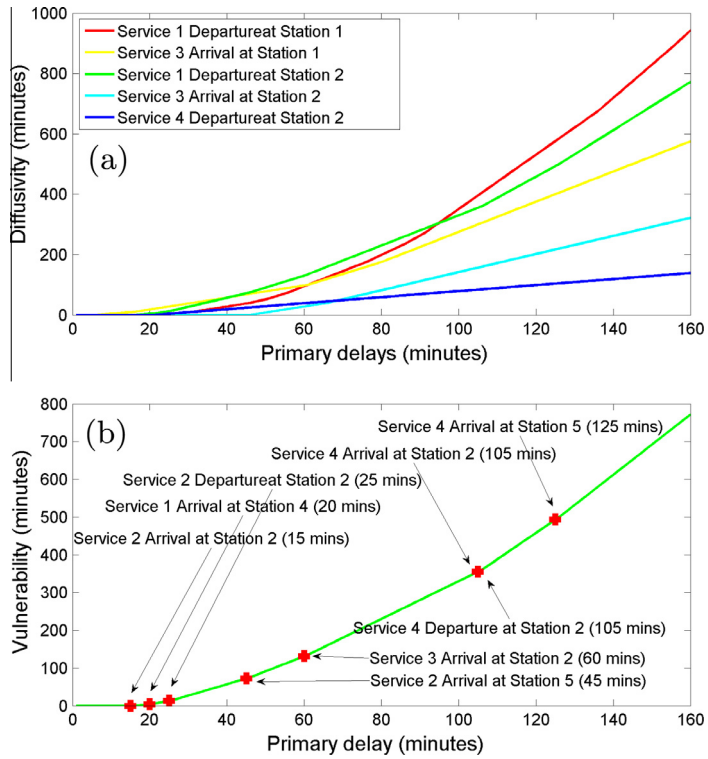


Fig. 9. (a) Diffusivity of arrivals and departures in the artificial railway network and (b) diffusivity of the departure of service 1 at station 2.

Table 4  
Primary delays under the cyclic timetable (in minutes).

Events	Simulation results	Iterative algorithm	APCP algorithm
Service 1 Arrival at Station 2 (Train 1)	155	155	155
Service 1 Arrival at Station 2 (Train 2)	115	115	115
Service 3 Arrival at Station 2 (Train 1)	95	95	95
Service 1 Arrival at Station 2 (Train 3)	80	80	80
Service 3 Arrival at Station 2 (Train 2)	70	70	70
Service 2 Arrival at Station 5 (Train 1)	187	187	187
Service 1 Arrival at Station 2 (Train 4)	55	55	55
Service 2 Arrival at Station 5 (Train 2)	132	132	132
Service 4 Arrival at Station 5 (Train 1)	102	102	102
Service 2 Arrival at Station 5 (Train 3)	82	82	82
Service 4 Arrival at Station 5 (Train 2)	52	52	52
Service 2 Arrival at Station 5 (Train 4)	32	32	32

Table 5  
Primary and secondary delays of service 1 under the cyclic timetable (in minutes).

Events	Simulation results	Iterative algorithm	APCP algorithm
Arrival at Station 2 (Train 1)	155	155	155
Departure at Station 2 (Train 1)	145	145	145
Arrival at Station 2 (Train 2)	115	115	115
Departure at Station 2 (Train 2)	105	105	105
Departure at Station 2 (Train 3)	80	80	80
Arrival at Station 4 (Train 1)	125	125	125
Departure at Station 2 (Train 3)	70	70	70
Arrival at Station 4 (Train 4)	55	55	55
Departure at Station 2 (Train 4)	45	45	45
Arrival at Station 4 (Train 2)	85	85	85
Arrival at Station 2 (Train 5)	30	30	30
Arrival at Station 4 (Train 3)	50	50	50
Departure at Station 2 (Train 5)	20	20	20

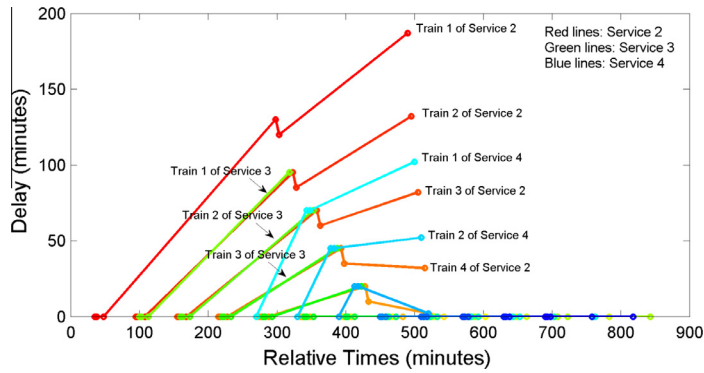


Fig. 10. Delays of service 2, 3 and 4 under the cyclic timetable.

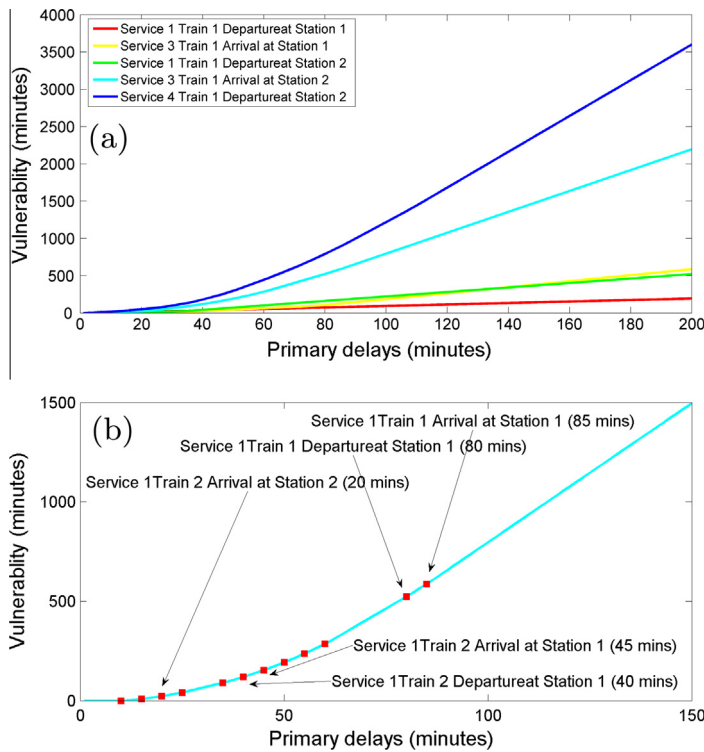


Fig. 11. (a) Vulnerabilities of arrivals and departures in the artificial railway network and (b) vulnerability of the arrival of train 1 in service 3 at station 2.

4.1.1. Case study on an artificial network with an acyclic timetable

Assume the services operate according to an acyclic timetable listed in Table 2. Each service only operates once for 24 h. The slack time matrix  $B^{(0)}$  and the APCP matrix are shown in Appendix B. The results from the APCP algorithm are listed in Table 3, which are exactly the same as the outputs from the iterative algorithm and the simulation program.

As we can see from the results, the inclement weather has caused primary delays on all the services. The arrival of service 1 at station 2 incurs a primary delay of 155 min due to the reduced operating speed between station 1 and station 2 at the first stage of the inclement weather. This primary delay propagates to the subsequent events of service 1, service 2 and service 4 with gradually reduced intensity. For example, the slack time between the arrival and departure of service 1 at station 2 is 10 min, therefore, the departure delay of service 1 at station 2 is reduced to 145 min. The arrival of service 2 at station 5 incurs the most severe delay of 187 min. This is the result of both the secondary departure delay at station 2 and the additional primary delay due to the inclement weather between station 2 and station 5.

The vulnerabilities of selected services under the acyclic timetable are plotted in Fig. 8. As we can see, the vulnerability increases with the primary delay in a piecewise manner, which agrees with the mathematical structure of Eq. (45). Taking the departure of service 1 at station 2 as an example, its vulnerability is composed of four segments, separated at points of

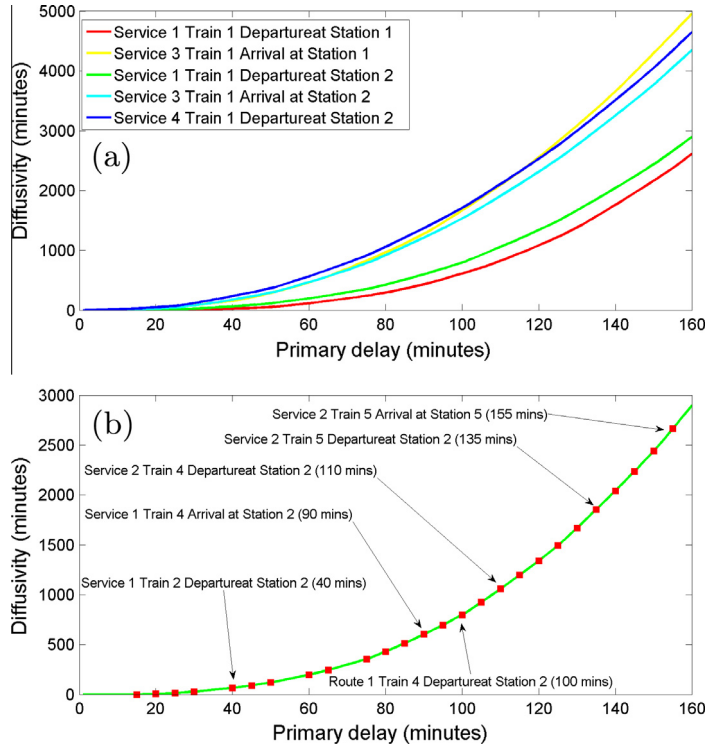


Fig. 12. (a) Diffusivity of arrivals and departures in the artificial railway network and (b) diffusivity of the departure of train 1 in service 1 at station 2.

10, 30 and 35, which are equal to  $\omega_s(7, 8)$ ,  $\omega_s(2, 8)$  and  $\omega_s(1, 8)$  in the APCP graph, respectively. When the primary delay  $d^*$  is between 10 and 30 min, only  $\omega_s(7, 8) \otimes d^*$  is positive and thus we have  $U_i(d^*) = -10 \otimes d^*$ , which corresponds to the first segment of the vulnerability curve in Fig. 8b.

The diffusivities of selected events are plotted in Fig. 9a. Similarly, the diffusivity increases with the intensity of the primary delay in a piecewise manner since Eq. (43) has a similar structure as Eq. (45). As shown in Fig. 9b, the diffusivity of the departure of service 1 at station 2 is composed of 8 segments, separated by points of 15, 20, 25, 45, 60, 105 and 125, which can be found from the eighth column of the APCP matrix. When the primary delay is below 15 min, it does not propagate to any other event and its diffusivity equals zero. When the primary delay is between 15 and 20 min, it will affect the arrival of service 2 at station 2. Similarly, each point of discontinuity in the curve indicates an additional arrival or departure event is affected by the primary delay.

#### 4.1.2. Case study on an artificial network with a cyclic timetable

In this section, the proposed model is validated under a cyclic timetable. We assume the periodicity is 1 h for each service. The departure and arrival times of the last train of each service are as follows:

- The last train of service 1 departs from station 1 at 18:20 and arrives at station 4 at 20:35.
- The last train of service 2 departs from station 3 at 18:55 and arrives at station 5 at 21:10.
- The last train of service 3 departs from station 1 at 20:00 and arrives at station 2 at 21:50.
- The last train of service 4 departs from station 2 at 20:45 and arrives at station 5 at 22:45.

Assume the network is subjected to the same two-stage inclement weather as introduced in the previous section. The resulting primary delays are listed in Table 4. Secondary delays of service 1 are listed in Table 5, while delays of other services are plotted in Fig. 10. The consistency among the results from the APCP algorithm, the iterative algorithm and the simulation program again proved the validity of the SMPS model and the APCP algorithm under cyclic timetables.

As shown in Table 4, in our example, the inclement weather has resulted in much more severe delays under the cyclic timetable compared to the acyclic one due to more frequent services and more strict constraints. For example, four trains in service 1 have incurred primary delays upon arrival at station 2, which result in a total of 13 secondary delays in service 1. It is noteworthy that, in a periodic timetable, a primary delay could propagate to successive trains in the same service. For example, the arrival of train 5 of service 1 at station 2 is delayed due to the knock-on impact from the preceding train, i.e., train 4, in the same service. The propagation of primary delays can also be clearly identified from Fig. 10. The arrivals of

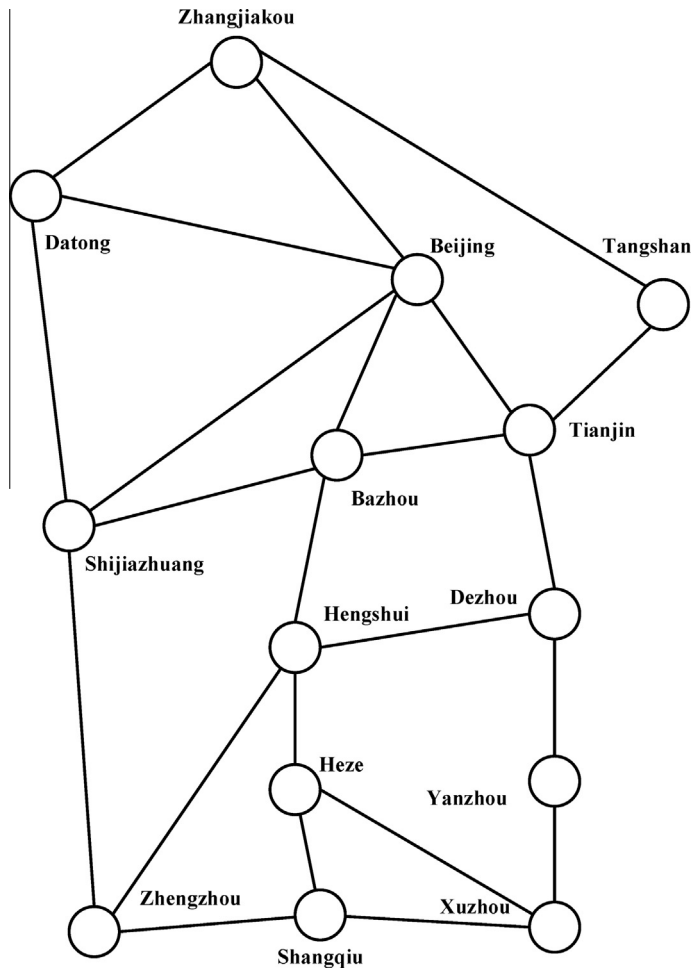


Fig. 13. An empirical regional network in northern China.

**Table 6**

Primary delays in the empirical network in scenario 1 (in minutes).

Events	Simulation results	Iterative algorithm	APCP algorithm
K148 Arrival at BeijingXi	67	67	67
K974 Arrival at Bazhou	191	191	191
K126 Arrival at Bazhou	110	110	110
K106 Arrival at Bazhou	75	75	75
K546 Arrival at Bazhou	55	55	55
K600 Arrival at Shijiazhuang	195	195	195
K370 Arrival at Shijiazhuang	214	214	214
K386 Arrival at Shijiazhuang	205	205	205

trains 1, 2, 3 and 4 in service 2 at station 2 are delayed due to the departure delays of multiple trains in service 1. However, the severity of the delay propagation is not necessarily linked to the periodicity of the timetable. Instead, it should be examined on a case-by-case basis.

Compared with the acyclic timetable, the arrival and departure events under the cyclic timetable are much more vulnerable, as shown in Fig. 11. This is easy to understand since more frequent services result in more strict constraints. For example, as shown in Fig. 11b, the arrival of the first train of service 3 will be affected by a total of 12 events if the primary delay exceeds 80 min. Similarly, arrivals and departures in a cyclic timetable also tend to be more diffusive as shown in Fig. 12. Nevertheless, the vulnerability and diffusivity of an event in a cyclic timetable are not necessarily greater than that in an acyclic timetable.

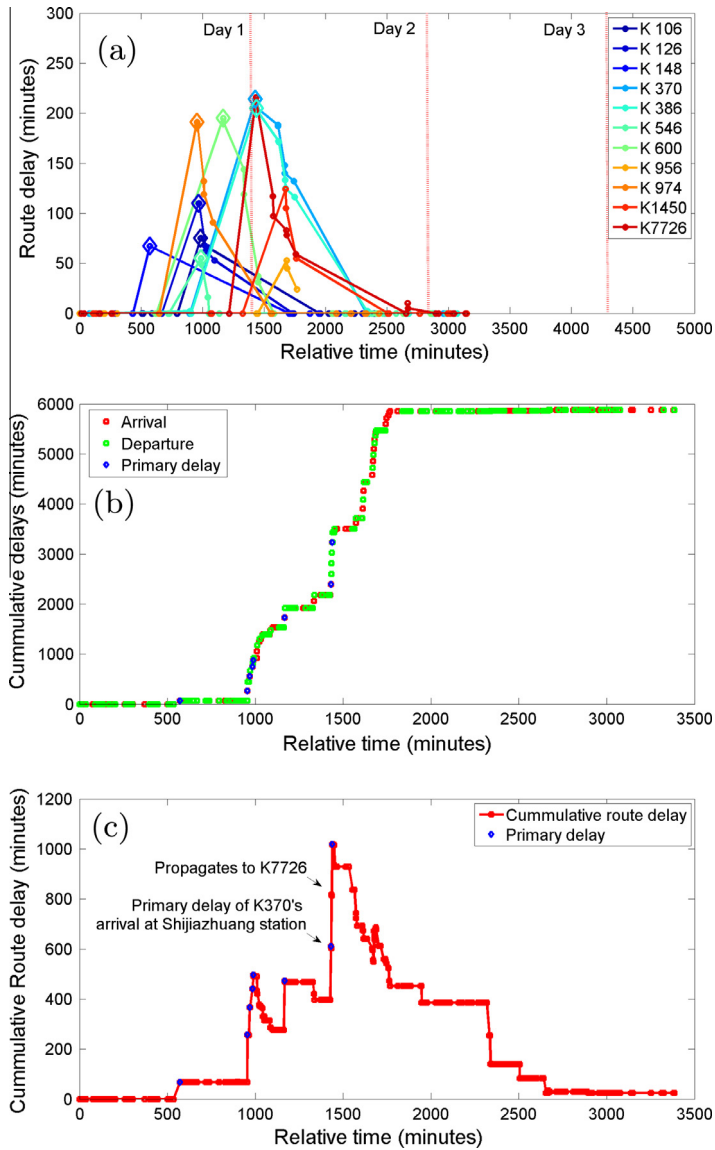


Fig. 14. (a) Service delays in the empirical railway network; (b) cumulative secondary delays in the empirical railway network; and (c) cumulative secondary delays grouped by service in the empirical railway network.

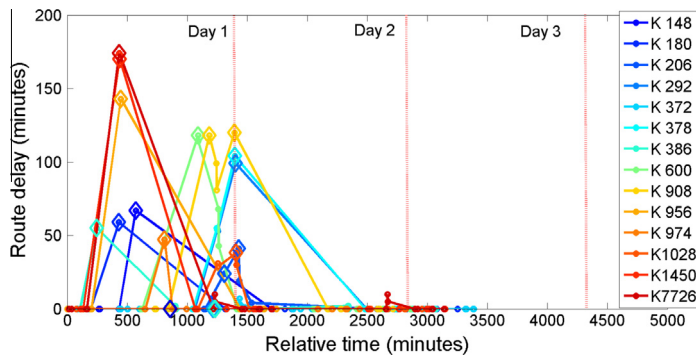


Fig. 15. Service delays in the empirical railway network in scenario 2.

**Table 7**

Specifications of the inclement weather in scenarios 2 and 3.

No.	Periods in scenario 2	Periods in scenario 3	Affected links	Maximum operating speed (km/h)
1	3:00–6:00	3:00–11:00	Between Datong and Zhangjiakou; Between Beijing and Zhangjiakou; Between Tangshan and Zhangjiakou; Between Tianjin and Tangshan	20
2	6:00–9:00	11:00–20:00	Between Datong and Beijing; Between Beijing and Tianjin; Between Bazhou and Beijing; Between Bazhou and Tianjin; Between Beijing and Shijiazhuang	20
3	8:00–12:00	20:00–3:00 (2nd day)	Between Bazhou and Shijiazhuang; Between Henghui and Bazhou; Between Dezhou and Tianjin	20
4	12:00–14:00	3:00–11:00 (2nd day)	Between Shijiazhuang and Zhenzhou; Between Hengshui and Dezhou; Between Dezhou and Yanzhou	30
5	14:00–17:00	11:00–15:00 (2nd day)	Between Hengshui and Zhengzhou; Between Hengshui and Heze; Between Yanzhou and Xuzhou	40
6	17:00–21:00	15:00–23:00 (2nd day)	Between Xuzhou and Heze; Between Heze and Shangqiu; Between Shangqiu and Zhenzhou Between Shangqiu and Xuzhou	50

**Table 8**

Primary delays in the empirical network in scenario 2 (in minutes).

Events	Simulation results	Iterative algorithm	APCP algorithm
K386 Arrival at Tangshan	55	55	55
K7726 Arrival at Tangshan	174	174	174
K1450 Arrival at Tangshan	170	170	170
K956 Arrival at Tangshan	143	143	143
K180 Arrival at BeijingXi	59	59	59
K148 Arrival at BeijingXi	67	67	67
K974 Arrival at Bazhou	47	47	47
K600 Arrival at Shijiazhuang	118	118	118
K908 Arrival at Heze	118	118	118
K908 Arrival at Xuzhou	120	120	120
K206 Arrival at Shangqiu	24	24	24
K378 Arrival at Xuzhou	104	104	104
K292 Arrival at Xuzhou	99	99	99
K1028 Arrival at Xuzhou	38	38	38
K206 Arrival at Xuzhou	41	41	41

**Table 9**

Primary delays in the empirical network in scenario 3 (in minutes).

Events	Simulation results	Iterative algorithm	APCP algorithm
K386 Arrival at Tangshan	55	55	55
K7726 Arrival at Tangshan	246	246	246
K1450 Arrival at Tangshan	242	242	242
K956 Arrival at Tangshan	268	268	268
K974 Arrival at Tianjing	151	151	151
K126 Arrival at Tianjing	165	165	165
K106 Arrival at BeijingXi	211	211	211
K546 Arrival at Tianjing	170	170	170
K600 Arrival at BeijingXi	127	127	127
K2286 Arrival at Tianjing	261	261	261
K370 Arrival at Bazhou	370	370	370
K386 Arrival at Bazhou (2nd train)	277	277	277
K1450 Arrival at Tianjing (2nd train)	229	229	229
K180 Arrival at Shijiazhuang	22	22	22
K956 Arrival at Tianjing (2nd train)	158	158	158
K372 Arrival at Dezhou	239	239	239
K126 Arrival at Shijiazhuang (2nd train)	147	147	147
K908 Arrival at Heze	9	9	9
K908 Arrival at Shangqiu	47	47	47
K378 Arrival at Shangqiu	103	103	103
K292 Arrival at Shangqiu	109	109	109
K1028 Arrival at Shangqiu	106	106	106
K908 Arrival at Xuzhou	95	95	95
K206 Arrival at Shangqiu	99	99	99
K378 Arrival at Xuzhou	130	130	130
K292 Arrival at Xuzhou	126	126	126
K1028 Arrival at Xuzhou	72	72	72

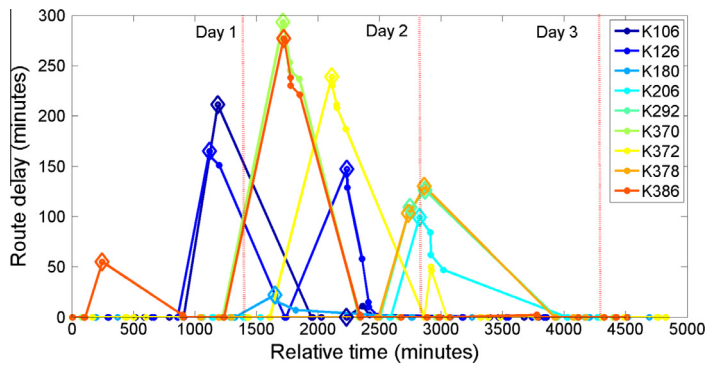


Fig. 16. Delays from selected services in the empirical railway network in scenario 3.

Table 10

Computation times of the APCP algorithm, the iterative and the simulation program (average of 10 runs, in seconds).

Computation time	APCP algorithm	Iterative algorithm	Simulation program
Scenario 1	1.51	2.12	40.87
Scenario 2	1.77	2.43	44.12
Scenario 3	1.90	2.78	50.21

## 4.2. Case study on an empirical network

This section presents a case study on a real-world railway network in northern China as shown in Fig. 13. The timetable and link distances are shown in Appendix C, which contains 14 stations and 22 selected services sharing the same railway links and platforms at stations. The speed limit in normal conditions is 100 km/h. The minimum arrival headway and the minimum departure headway are both 5 min. The minimum dwell time and the safety time at stations are assumed to be 2 min.

### 4.2.1. Delay propagation under inclement weather

In the first scenario, we assume the railway network is impacted by a three-stage inclement weather. The first stage begins at 3:00 and ends at 9:00, during which the maximum operating speeds on the links between Bazhou Station and Tianjing Station and between Bazhou Station and Beijing Station have to be reduced to 30 km/h. The second stage begins at 9:00 and ends at 15:00, during which the maximum operating speeds on the links between Henghui Station and Bazhou Station and between Shijiazhuang Station and Bazhou Station have to be reduced to 30 km/h. In the third stage that starts at 15:00 and ends at 21:00, the inclement weather has the same intensity and affects the links between Shijiazhuang Station and Hengshui Station and between Zhengzhou Station and Hengshui Station.

A total of eight primary delays occur as listed in Table 6. The primary delays of K148, K974, K126, K106, K546 and K600 are gradually recovered by slack times and do not propagate to any other services as shown in Fig. 14a. However, K370's primary delay at Shijiazhuang Station causes a secondary delay on K7726 since the arrival of K7726 at Tianjin Station is scheduled after K370's arrival. Similarly, the primary delay of K386 propagates to K1450 due to the safety time constraint at Tianjin Station (see Fig. 15).

Fig. 14b and c further shows the cumulative delays of the railway network. In Fig. 14b, the cumulative delay is the sum of the delays of all departures and arrival events. As one can see from the figure, once a primary delay occurs, the cumulative delay will increase first and then remain stable after the primary delay being absorbed by slack times. Fig. 14c shows the cumulative delays grouped by service. For example, when the primary delay of K370 causes a secondary delay on K7726, the cumulative delay sharply increases at first and then gradually decreases due to slack times. After all the primary delays being absorbed, all services return to the scheduled timetable.

To show the delay propagation in more complex scenarios, we extend the inclement weather with larger spatial-temporal coverages. The time periods, the spatial coverages, and the maximum operating speeds are listed in Table 7. The inclement weather in both extended scenarios includes six stages that last for 18 and 44 h, respectively.

The primary delays in the second scenario are listed in Table 8. A total of 15 arrival and departure events in 14 services have incurred primary delays, resulting in 27 knock-on delays over the network. Compared with the first scenario, more services have incurred primary delays due to the larger spatial coverage of the inclement weather. Some services suffer both primary and secondary delays. For example, due to the departure delay of K292, K1028 incurs a secondary delay of 31 min when arriving at Shangqiu Station. However, after it departs from the station, the operating speed is reduced to 50 km/h due to the inclement weather from 21:00 to 23:00, and consequently, it suffers another primary delay of 38 min.

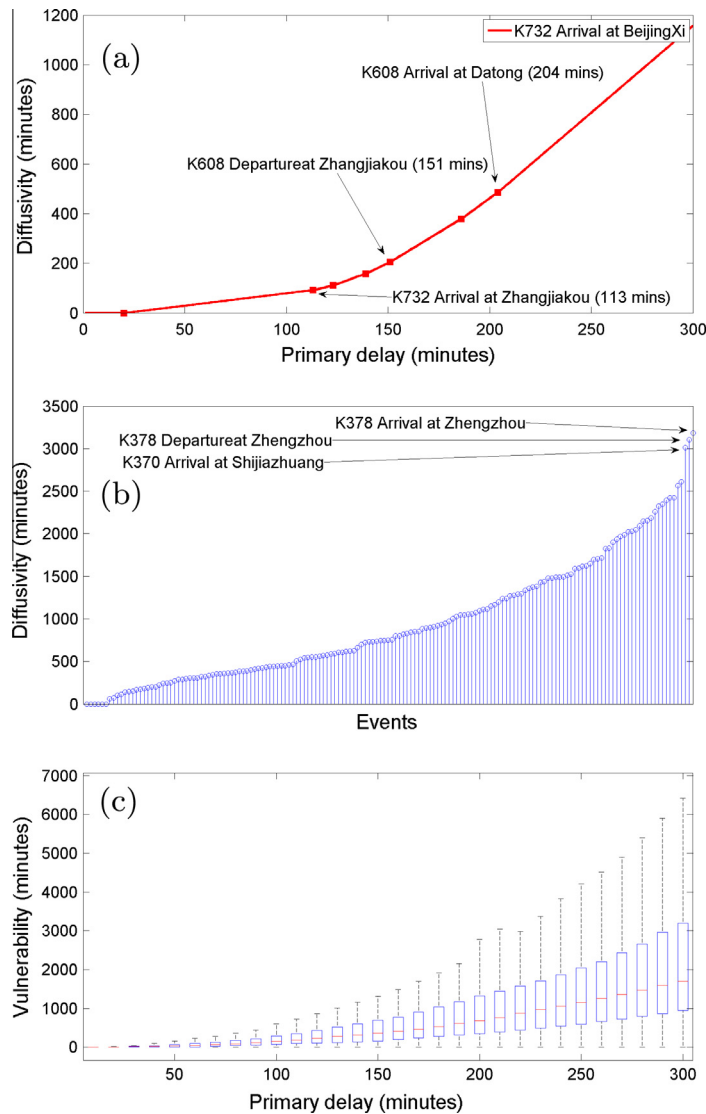


**Fig. 17.** (a) Diffusivity of K732's arrival at BeijingXi; (b) diffusivities of arrivals and departures for the real-world railway network with a primary delay of 200 min; and (c) Boxplot of diffusivities of arrivals and departures.

In the third scenario, the inclement weather lasts for 44 h. A total of 27 arrival and departure events in 17 services have incurred primary delays, resulting in 104 knock-on delays. The primary delays are listed in Table 9. Delays of selected services are plotted in Fig. 16. It is noteworthy that because of the extended duration of the inclement weather, multiple trains in a service on consecutive days could be affected. For example, K386 incurs primary delays in two consecutive days because of the inclement weather at the first and third stages. The primary delays obviously have more profound impacts on the network, and their propagation cannot be fully eliminated until the end of the third day.

The above experiments for the empirical network are performed on a workstation configured with Intel Core i7 2.67 GHz and 8 Gb RAM. The computation times of the APCP algorithm, the iterative algorithm, and the simulation program are listed in Table 10. The APCP graph was computed using the QuickGraph package (De Halleux, 2007). It is apparent that the simulation program is the most time consuming since it has to simulate movements of trains at each time step (1 s in our experiments). Not surprisingly, the APCP algorithm outperforms the iterative algorithm in all three scenarios by 50%. The advantage is expected to be more significant for railway networks with more frequent services as implied by the time complexities in Eqs. (42) and (49).

#### 4.2.2. Vulnerability and diffusivity of the empirical network

As pointed out in the artificial network case, both vulnerability and diffusivity increase with the intensity of the primary delay in a piecewise manner. Fig. 17a plots the diffusivity of the arrival of K732 at Beijing Station, which is composed of

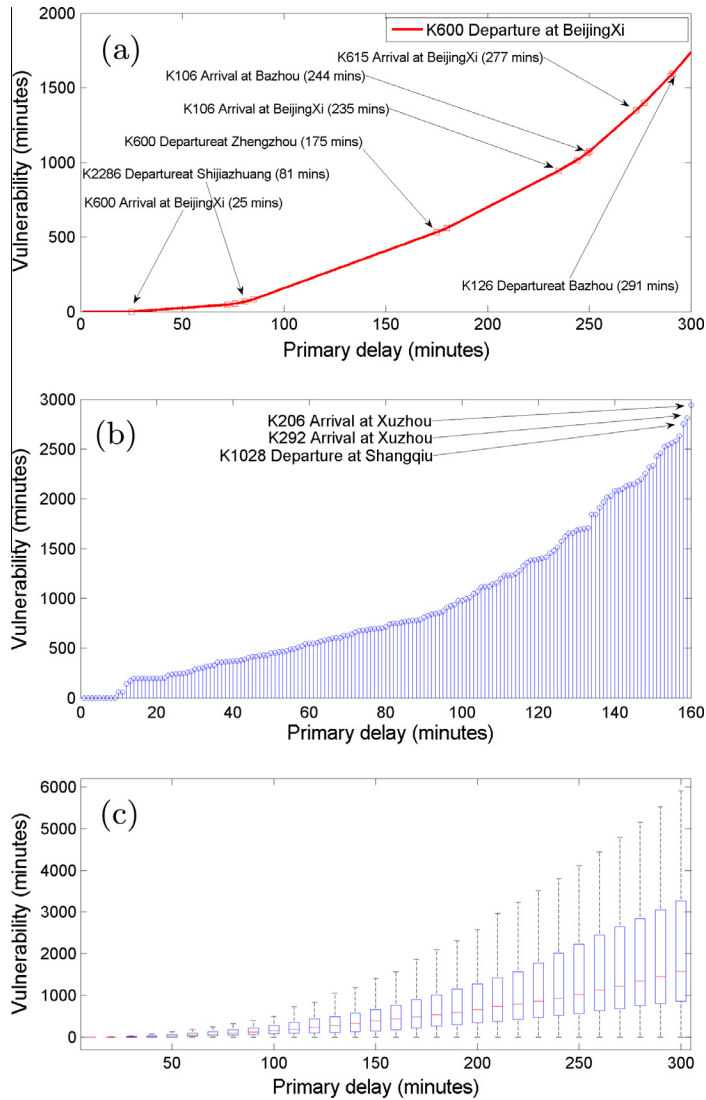


**Fig. 18.** (a) Vulnerability of K600's departure at BeijingXi; (b) vulnerability of arrivals and departures for the real-world railway network with a primary delay of 200 min; and (c) Boxplot of vulnerability of arrivals and departures.

multiple linear segments. Each point of discontinuity in the curve indicates that the primary delay propagates to an additional departure or arrival. For example, when the primary delay exceeds 151 min, the delay propagates to the departure of K608 at Zhangjiakou Station since the weight of the critical path to this event is  $-151$  in the APCP graph. Fig. 17b further shows the diffusivities of all events given a primary delay of 200 min and the most diffusive event is the arrival of K370 at Zhengzhou Station. It indicates that if this event incurs a primary delay of 200 min, it would cause the most severe secondary delays over the network.

Fig. 17c shows the box-plot of the diffusivities of all arrivals and departures. It can be seen that with the growth of the primary delay, both the median and the largest diffusivities increase. The box-plot also indicates that the distribution of the diffusivity is asymmetric and skewed to the larger values. Moreover, the growth of secondary delays is clearly faster than a linear growth. Similarly, vulnerability also increases with the primary delay in a piecewise manner, as shown in Fig. 18a. For example, when the primary delay of K106's departure at Zhengzhou Station exceeds 235 min, the departure of K600 at Beijing Station will be affected due to the limited slack time between these two events. If the primary delay exceeds 291 min, a total of 15 events can propagate their primary delays to this departure event, as can be seen in Fig. 18a.

The vulnerabilities of all arrivals and departures under a primary delay of 200 min are shown in Fig. 18b. The most vulnerable event is the arrival of K206 at Xuzhou Station. It indicates that, when a primary delay of 200 min is imposed on other events, the arrival of K206 at Xuzhou Station is the most susceptible event and would incur the largest secondary delay. The box-plots for vulnerabilities of all arrivals and departures are shown in Fig. 18c. The median and the largest

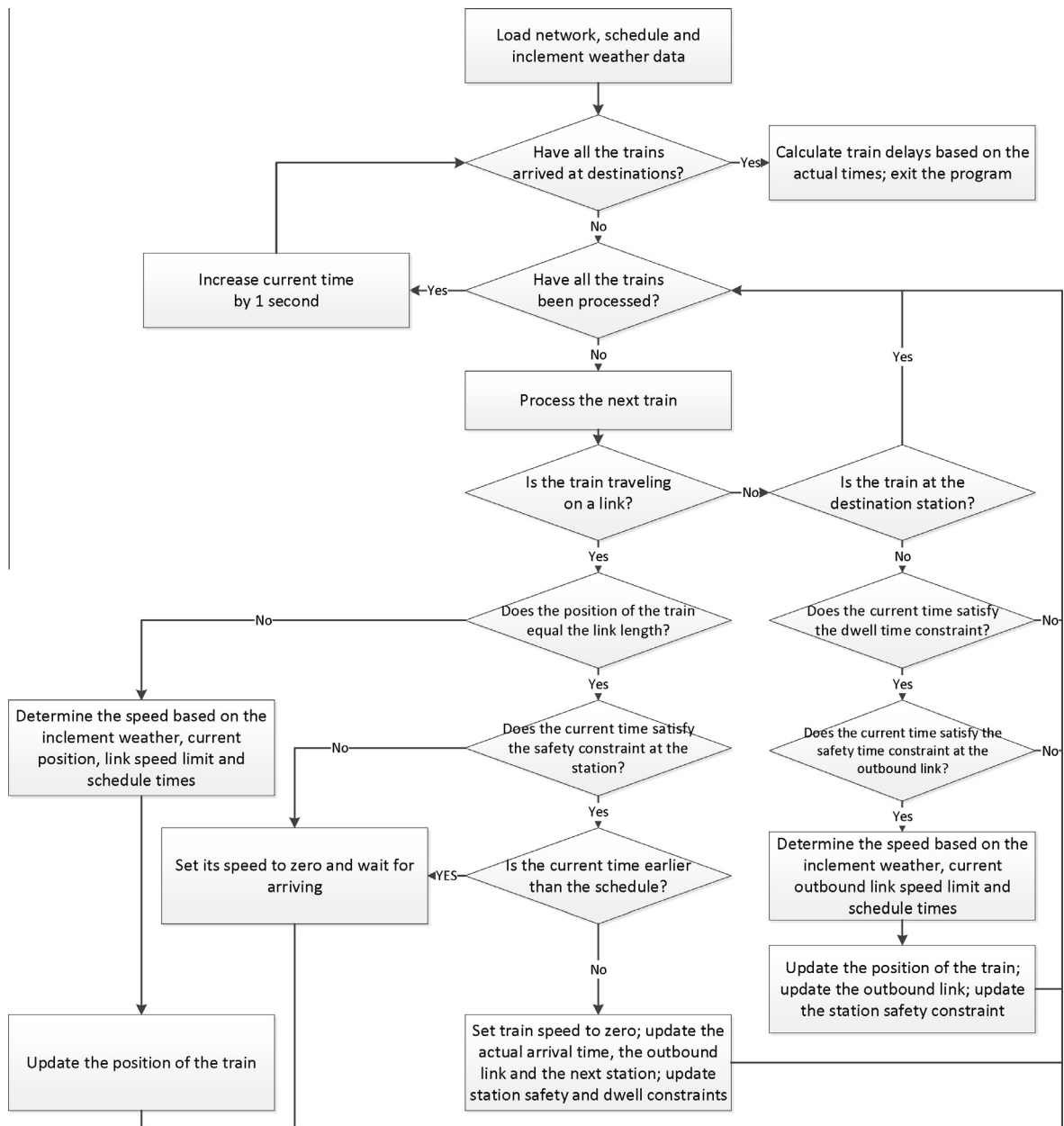


Fig. A.19. Work-flow of the simulation program.

vulnerabilities increase with the primary delay. The distribution shown in the box-plot is also asymmetric and skewed to the larger values. The growth of the vulnerability is faster than a linear growth rate, which can be easily understood from the nonlinearity of Eq. (45).

## 5. Conclusion

This paper presented an SMPS model to capture the cascade dynamics of delay propagation on railway networks under inclement weather. The APCP algorithm was developed to solve the SMPS model with improved computational efficiency. The SMPS model and the APCP algorithm were tested on both artificial and empirical railway networks. The results indicated that the SMPS model is a viable method to predict delay propagation on railway networks under inclement weather. The APCP algorithm is able to successfully solve the SMPS system. The experiments have also shown that the APCP algorithm is much more efficient than the discrete-time simulation program. The improved efficiency is

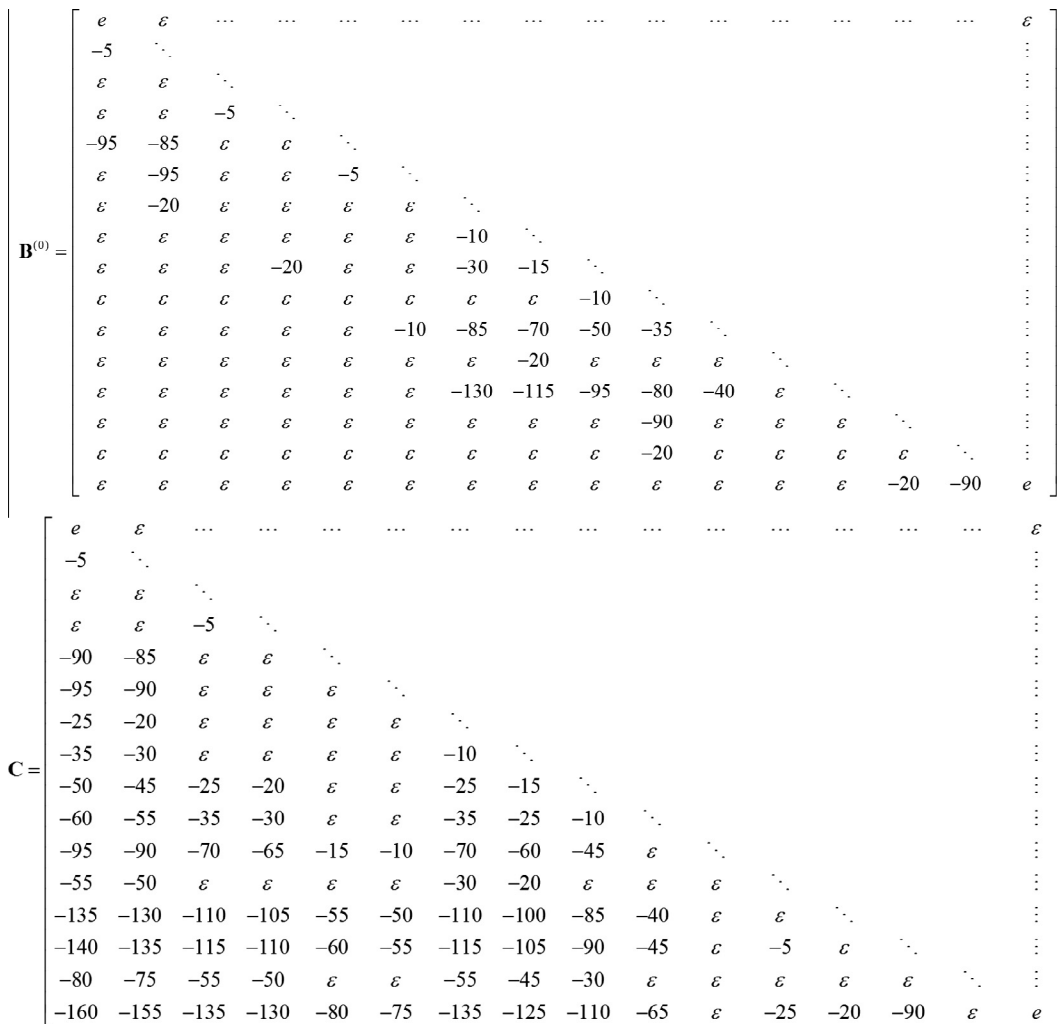


Fig. B.20. (a) Slack time matrix and (b) APCP matrix.

particularly valuable for predicting delay propagation in larger-scale networks with busy services. More importantly, based on the APCP graph, the robustness of railway services can be readily evaluated using the concepts of vulnerability and diffusivity.

Compared to the classical MPS (Braker, 1993; Subiono, 2000; Goverde, 2007), the new model is able to incorporate multiple system matrices so as to capture the dynamic impacts of inclement weather. Delays obtained from the proposed model can be utilized for proactive train re-scheduling and management. The vulnerability and the diffusivity derived from the APCP graph can be applied as key performance measures to design resilient timetables.

Based on the proposed model, the future work will be focused in two directions. On the one hand, proactive railway re-scheduling models can be developed to alleviate the interruptions of inclement weather by minimizing train and travel delays. In these control models, the proposed SMPS can serve as the basic system dynamic model, and various control strategies, e.g., predictive control, can be applied. On the other hand, the proposed model, particularly the APCP graph and the robustness measures, can be further utilized to design robust timetables that are able to withstand the propagation of disturbances.

### Acknowledgments

The research is partially sponsored by the Chinese Nature Science Foundation through the project No. 61374157. The authors are grateful to the anonymous referees for their detailed comments and suggestions, which greatly improved the quality and clarity of the paper.

**Table C.11**  
Timetable of the regional railway network.

Station	Arrival time	Departure time	Distance (km)
<i>K600</i>			
Zhengzhou		10:30	0
Shijiazhuang	16:16	16:22	412
Beijing	19:55	20:22	277
Zhangjiakou	23:38	23:46	190
Datong	2:24		178
<i>K180</i>			
Zhengzhou		22:12	0
Shijiazhuang	3:13	3:21	412
Beijing	6:16		277
<i>K7726</i>			
Shijiazhuang		20:40	0
Beijing	0:20	0:42	277
Tianjin	2:42	2:50	127
Tangshan	4:23		123
<i>K370</i>			
Zhengzhou		15:02	0
Shijiazhuang	20:21	20:31	412
Bazhou	23:49	23:52	300
Tianjing	1:23	1:33	87
Tangshan	2:55		123
<i>K974</i>			
Zhengzhou		2:08	0
Hengshui	10:50	10:54	606
Bazhou	12:49	12:53	182
Tianjing	14:42	14:57	87
Tangshan	16:39		123
<i>K148</i>			
Hengshui		4:37	0
Bazhou	7:15	7:19	182
Beijing	8:28		92
<i>K732</i>			
Hengshui		6:53	0
Bazhou	8:59	9:01	182
Beijing	10:02	10:24	92
Zhangjiakou	13:51	14:03	190
Datong	16:53		178
<i>K615</i>			
Beijing		15:40	0
Zhangjiakou	18:52	19:02	190
Datong	21:48		178
<i>K608</i>			
Tianjin		8:42	0
Zhangjiakou	14:02	14:13	299
Datong	17:06		178
<i>K386</i>			
Zhenzhou		15:10	0
Shijiazhuang	20:38	20:42	412
Bazhou	0:09	0:13	300
Tianjin	1:43	1:53	87
Tangshan	3:16		123
<i>K1450</i>			
Yanzhou		18:00	0
Dezhou	22:09	22:12	249
Tianjin	1:56	2:18	224
Tangshan	4:32		134
<i>K956</i>			
Dezhou		0:14	0
Tianjin	3:17	3:28	225
Tangshan	5:03		123
<i>K126</i>			
Zhenzhou		5:05	0
Shijiazhuang	10:53	11:13	412

Table C.11 (continued)

Station	Arrival time	Departure time	Distance (km)
Bazhou	14:23	14:25	198
Tianjin	16:00	16:07	87
Tangshan	17:30		123
<i>K106</i>			
Shangqiu		8:39	0
Heze	9:51	9:53	95
Hengshui	13:17	13:20	105
Bazhou	15:14	15:16	182
Beijingxi	16:20		92
<i>K546</i>			
Shijiazhuang		12:13	0
Bazhou	15:38	15:46	198
Tianjin	17:11	17:37	87
Tangshan	18:59		123
<i>K908</i>			
Shijiazhuang		12:23	0
Hengshui	14:02	14:08	99
Heze	17:50	17:52	222
Shangqiu	19:08	19:28	76
Xuzhou	21:17		109
<i>K2286</i>			
Shijiazhuang		16:09	0
Hengshui	17:46	17:52	122
Dezhou	18:42	19:07	62
Tianjin	23:03	23:09	239
Tangshan	0:30		123
<i>K378</i>			
Zhenzhou		17:48	0
Shangqiu	20:02	20:06	203
Xuzhou	21:48		146
<i>K1028</i>			
Zhenzhou		18:13	0
Shangqiu	20:30	20:35	203
Xuzhou	22:54	23:14	146
Yanzhou	1:20		173
<i>K206</i>			
Zhenzhou		19:15	0
Shangqiu	20:30	21:32	203
Xuzhou	23:14	23:38	146
Yanzhou	1:37		173
<i>K292</i>			
Zhenzhou		17:48	0
Shangqiu	20:02	20:06	203
Xuzhou	21:48		146
<i>K372</i>			
Xuzhou		23:59	0
Yanzhou	2:51	2:55	163
Dezhou	7:18	7:29	274
Hengshui	8:25	8:30	62
Shijiazhuang	10:04		122

## Appendix A. The work-flow chart of the simulation program

A discrete-time simulation program was developed using the C-sharp language to validate the SMPS model and its solution algorithm. The program first reads the input data from a Microsoft Access Database, including the network data, the inclement weather information and the timetable. After the objects of trains, stations and links being initialized, the simulation will iteratively calculate train movements until all the trains have arrived at the destinations. The arrival and departure times are recorded at each stations to compute train delays. In each time step, the train speed is updated based on the safety constraints and the operating speed limit. A Boolean signal variable is designed in the programmatic objects of stations to indicate whether the safety constraints are satisfied. For example, when a train departs from a station, the signal variable is set to false and will not be set back to true until a period that is larger than the safety time at stations has elapsed.

The arrival and departure headway constraints are implemented similarly. Details of the simulation process are described in the work-flow in Fig. A.19.

## Appendix B. Slack-time matrix and ACPG graph of the artificial network with an acyclic timetable

The slack time matrix and the ACPG matrix for the acyclic timetable in the artificial network are shown in Fig. B.20.

## Appendix C. The timetable of the regional railway network

The timetable of the regional railway network is listed in Table C.11.

## References

- Bacelli, F., Cohen, G., Olsder, G.J., Quadrat, J., 1992. *Synchronization and Linearity*. John Wiley & Sons, New York, USA.
- Braker, J., 1993. *Algorithms and Applications in Timed Discrete Event Systems*. Ph.D. Thesis, Department of Technical Mathematics and Informatics, Delft University of Technology.
- Butkovic, P., 2010. *Max-linear Systems: Theory and Algorithms*. Springer-Verlag, London, UK.
- Cacchiani, V., Galli, L., Toth, P., 2014. A tutorial on non-periodic train timetabling and platforming problems. *EURO J. Transport. Logist.*, 1–36 <http://dx.doi.org/10.1007/s13676-014-0046-4>.
- Caimi, G., Laumanns, M., Schüpbach, K., Wörner, S., Fuchsberger, M., 2011. The periodic service intention as a conceptual framework for generating timetables with partial periodicity. *Transport. Plann. Technol.* 34 (4), 323–339.
- Canca, D., Barrena, E., Algaba, E., Zarzo, A., 2014. Design and analysis of demand-adapted railway timetables. *J. Adv. Transport.* 48 (2), 119–137.
- Carey, M., Kwicinski, A., 1994. Stochastic approximation to the effects of headways on knock-on delays of trains. *Transport. Res. Part B: Methodol.* 28 (4), 251–267.
- China Meteorological Administration, 2007. *Rail Transportation Weather Ratings*. No. QX/T 101-2007. China Meteorological Administration.
- Chou, J.S., Kim, C., Kuo, Y.C., Ou, N.C., 2011. Deploying effective service strategy in the operations stage of high-speed rail. *Transport. Res. Part E: Logist. Transport. Rev.* 47 (4), 507–519.
- Cui, T., Zhang, W., 2010. Study on safety of train in side wind with changing attitudes. *J. China Railway Soc.* 32 (5), 507–519.
- De Halleux, J., 2007. Quickgraph: A 100% c# Graph Library with Graphviz Support. <<https://quickgraph.codeplex.com/>>.
- De Schutter, B., van den Boom, T., 2002. Connection and speed control in railway systems – a model predictive control approach. In: Silva, M., Giua, A., Colom, J. (Eds.), *Proceedings of the Sixth International Workshop on Discrete Event Systems*. Zaragoza, Spain, pp. 49–54.
- Floyd, R.W., 1962. Algorithm 97: shortest path. *Commun. ACM* 5 (6), 345.
- Forsgren, M., Aronsson, M., Kreuger, P., Dahlberg, H., 2011. The maraca: a tool for minimizing resource conflicts in a non-periodic railway timetable. In: Hansen, I., Wendler, E., Ricci, S., Pacciarelli, D., Longo, G., Rodriguez, J. (Eds.), *Proceedings of the 4th International Seminar on Railway Operations Research*. Roma, Italy, pp. 16–18.
- Goverde, R.M., 2007. Railway timetable stability analysis using max-plus system theory. *Transport. Res. Part B: Methodol.* 41 (2), 179–201.
- Higgins, A., Kozan, E., 1998. Modeling train delays in urban networks. *Transport. Sci.* 32 (4), 346–357.
- Johnson, D.B., 1977. Efficient algorithms for shortest paths in sparse networks. *J. ACM* 24 (1), 1–13.
- Kliwer, N., Suhl, L., 2011. A note on the online nature of the railway delay management problem. *Networks* 57 (1), 28–37.
- Ma, S., Ma, Y., Cheng, X., Ge, F., Li, Z., Zhang, J., Liu, Z., 2011. Determining method and risk assessment of strong wind region along high-speed railway in China. *J. Railway Eng. Soc.* 3 (1), 37–45.
- Meester, L.E., Muns, S., 2007. Stochastic delay propagation in railway networks and phase-type distributions. *Transport. Res. Part B: Methodol.* 41 (2), 218–230.
- Subiono, 2000. *On Classes of Min-Max-Plus Systems and Their Applications*, vol. 2/2000. IOS Press, Delft, The Netherlands.
- van den Boom, T.J., De Schutter, B., 2006. Modelling and control of discrete event systems using switching max-plus-linear systems. *Control Eng. Pract.* 14 (10), 1199–1211.
- van der Meer, D., 2008. *Modeling Railway Dispatching Actions in Switching Max-plus Linear Systems*. Master's Thesis, Department of Civil Engineering, Delft University of Technology.
- Warshall, S., 1962. A theorem on boolean matrices. *J. ACM* 9 (1), 11–12.
- Wong, R.C., Yuen, T.W., Fung, K.W., Leung, J.M., 2008. Optimizing timetable synchronization for rail mass transit. *Transport. Sci.* 42 (1), 57–69.
- Zeng, A.Z., Durach, C.F., Fang, Y., 2012. Collaboration decisions on disruption recovery service in urban public tram systems. *Transport. Res. Part E: Logist. Transport. Rev.* 48 (3), 578–590.
- Zheng, J., 2010. Railway passenger transportation development in China. *Urban Transp. China* 8 (1), 14–19.
- Zhou, X., Zhong, M., 2007. Single-track train timetabling with guaranteed optimality: branch-and-bound algorithms with enhanced lower bounds. *Transport. Res. Part B: Methodol.* 41 (3), 320–341.